Journal of Medicinal Chemistry



Article

# The 1,2,4-Triazolo[4,3-*a*]pyrazin-3-one as a Versatile Scaffold for the Design of Potent Adenosine Human Receptor Antagonists. Structural Investigations to Target the A Receptor Subtype

Matteo Falsini, Lucia Squarcialupi, Daniela Catarzi, Flavia Varano, Marco Betti, Diego Dal Ben, Gabriella Marucci, Michela Buccioni, Rosaria Volpini, Teresa De Vita, Andrea Cavalli, and Vittoria Colotta

*J. Med. Chem.*, **Just Accepted Manuscript** • Publication Date (Web): 07 Jun 2017

# The 1,2,4-Triazolo[4,3-*a*]pyrazin-3-one as a Versatile Scaffold for the Design of Potent Adenosine Human Receptor Antagonists. Structural Investigations to Target the $A_{2A}$ Receptor Subtype

Matteo Falsini,[a] Lucia Squarcialupi,[a] Daniela Catarzi,[a] Flavia Varano,[a] Marco Betti,[a] Diego Dal Ben,[b] Gabriella Marucci,[b] Michela Buccioni,[b] Rosaria Volpini,[b] Teresa De Vita,[c] Andrea Cavalli,[c,d] Vittoria Colotta[a*]

[a]*Dipartimento di Neuroscienze, Psicologia, Area del Farmaco e Salute del Bambino, Sezione di Farmaceutica e Nutraceutica, Università degli Studi di Firenze, Via Ugo Schiff, 6, 50019 Sesto Fiorentino, Italy.*

[b]*Scuola di Scienze del Farmaco e dei Prodotti della Salute, Università degli Studi di Camerino, via S. Agostino 1, 62032 Camerino (MC), Italy.*

[c]*CompuNet, Istituto Italiano di Tecnologia (IIT), Via Morego 30, 16163 Genova, Italy.*

[d]*Dipartimento di Farmacia e Biotecnologia, Università degli Studi di Bologna, Via Belmeloro 6, 40126 Bologna, Italy.*

**Key words**: G protein-coupled receptors, $A_{2A}$ adenosine receptor antagonists, 1,2,4-triazolo[4,3-*a*]pyrazin-3-one, ligand-adenosine receptor modeling studies.

## ABSTRACT

In this work we describe the identification of the 1,2,4-triazolo[4,3-*a*]pyrazin-3-one as a new versatile scaffold for the development of adenosine human (h) receptor antagonists. The new chemotype ensued from a molecular simplification approach applied to our previously reported 1,2,4-triazolo[4,3-*a*]quinoxalin-1-one series. Hence, a set of novel 8-amino-2-aryl-1,2,4-triazolopyrazin-3-one derivatives, featured by different substituents on the 2-phenyl ring (R) and at position 6 ($R_6$), was synthesized with the main purpose of targeting the $hA_{2A}$ adenosine receptor (AR). Several compounds possessed nanomolar affinity for the $hA_{2A}$ AR ($K_i$= 2.9-10 nM) and some, very interestingly, also showed high selectivity for the target. One selected potent $hA_{2A}$ AR antagonist (**12**, R= H, $R_6$= 4-methoxyphenyl) demonstrated some ability to counteract $MPP^+$-induced neurotoxicity in cultured human neuroblastoma SH-SY5Y cells, a widely used *in vitro* Parkinson's disease model. Docking studies at hAR structures were performed to rationalize the observed affinity data.

## INTRODUCTION

The neuromodulator--adenosine--exerts important physiological functions through activation of specific G protein-coupled receptors, subdivided into the four subtypes $A_1$, $A_{2A}$, $A_{2B}$ and $A_3$.[1,2] $A_{2A}$ adenosine receptor (AR) is ubiquitous in the human body and are expressed in a variety of peripheral organs such as the heart, liver and lung. In the central nervous system, a higher density of the $A_{2A}$ AR has been found in the striatum, nucleus accumbens and olfactory tuberculum and lower density in the cortex and hippocampus. $A_{2A}$ AR is highly expressed in platelets, leukocytes, immune and endothelial cells, implying a role of this receptor in the regulation of inflammatory processes.[1,2]

The $A_{2A}$ AR is coupled to Gs proteins that activate adenylate cyclase, thus enhancing intracellular cAMP levels. The subsequent stimulation of protein kinase A causes phosphorylation and activation of different proteins, such as receptors, enzymes and ion channels depending on the cell type and tissue. $A_{2A}$ AR has attracted much interest as druggable target for therapeutic intervention in neurodegenerative diseases,[3] such as Huntington's disease[4,5] and cerebral ischemia.[3,6,7] Related to them, the ability of $A_{2A}$ AR antagonists in inducing protection is well known and is largely attributed to the control of excessive glutamatergic transmission in striatal and nigral neurons, which prevents neuronal death.[4,7] A large body of evidence has clearly shown that $A_{2A}$ AR antagonists are beneficial in animal models of Parkinson's disease (PD)[8,9] and, as a result, pharmaceutical industries have progressed $A_{2A}$ antagonists to clinical trials, such as Istradefylline which has been approved for marketing in Japan.[10] $A_{2A}$ AR antagonists have demonstrated therapeutic value in the treatment of PD because they potentiate dopamine $D_2$ receptor-mediated neurotransmission. At a striatal level, in fact, the $A_{2A}$ AR is co-expressed with the $D_2$ dopamine receptor on GABAergic neurons of the indirect pathways of motor control where adenosine and dopamine elicit opposite effects in the modulation of adenylate cyclase activity, thus behaving as functional antagonists in the regulation of motor function.[11,12] Moreover, in the striatum, due to allosteric receptor-receptor interactions in the $A_{2A}$-$D_2$ heteroreceptor complexes, adenosine reduces

the affinity of agonists for the $D_2$ receptor, thus behaving as a negative modulator of $D_2$ receptor-mediated neurotransmission.[11-13]

However, interest in the use of $A_{2A}$ AR antagonists in PD has increased because recent studies have highlighted that, besides being effective in relieving motor symptoms, they might help control neuropsychiatric impairments of the disease, such as anxiety and cognitive deficiency[14,15] but, more importantly, help counteract neurodegeneration.[16,17] Although therapies are available to treat the signs and symptoms of PD, the progression of neuronal death remains relentless. Hence, there is a need to develop neuroprotective or disease-modifying treatments that stabilize this degeneration. In animal models, $A_{2A}$ AR antagonists protected nigral dopaminergic neurons from death induced by both 1-methyl-4-phenyl-1,2,3,6-tetrahydropyridine (MPTP) and 6-hydroxydopamine,[17] slowing the deterioration of dopamine-producing cells and modifying PD progression. However, the precise molecular mechanisms underlying the $A_{2A}$ AR blockade-induced neuroprotection is far from being clearly understood. Extra-striatal $A_{2A}$ ARs, e.g. those on the forebrain neurons, probably modulate neurodegeneration[18] and possibly exert protective effects mediated by extra-neuronal $A_{2A}$ ARs.[17] In particular, MPTP toxicity is probably attenuated through a mechanism counteracting neuroinflammation and involving $A_{2A}$ AR on glial cells.[17,19] MPTP is transformed into the toxic metabolite 1-methyl-4-phenyl-pyridinium ($MPP^+$) which produces cell death due to inhibition of mitochondrial respiratory chain.

Based on these data, most of our recent research in the field of adenosine[20-25] has been focused on identifying selective antagonists of the $hA_{2A}$ AR subtype. To this aim, different sets of 7-aminopyrazolo[4,3-*a*]pyrimidines have been synthesized recently[22,23,25] as bicyclic analogues of our tricyclic pyrazolo[3,4-*c*]quinoline derivatives[26,27] (Chart 1). The synthetic versatility of the bicyclic scaffold permitted us to replace the fused benzo ring of the leads with many different substituents (alkyl, aryl, arylalkyl) and to obtain several pyrazolo[4,3-*a*]pyrimidines endowed with nanomolar affinity for the $hA_{2A}$ receptor.[22,23] Hence, searching for a new bicyclic chemotype to develop selective $hA_{2A}$ AR antagonists, we applied the same simplification approach to another tricyclic

scaffold, i.e. the 1,2,4-triazolo[4,3-*a*]quinoxalin-1-one (Chart 1, TQX series) which we have successfully employed in the past to obtain potent and selective antagonists of $A_1$, $A_{2A}$ and $A_3$ ARs.[28-32] Thus, we designed the 2-aryl-8-amino-1,2,4-triazolo[4,3-*a*]pyrazin-3-one series (Chart 1) considering that its synthetic accessibility would have permitted us to introduce diverse substituents ($R_6$) with different lipophilic and steric properties at the 6-position. Hence, a set of 8-amino-1,2,4-triazolopyrazin-3-one derivatives (Chart 1, **1-26**) was synthesized and biologically assayed at hARs to investigate the SARs of this new series and to shed light on the structural requirements of targeting the $hA_{2A}$ AR subtype. Binding studies at hARs were also carried out on the intermediates 1,2,4-triazolo[4,3-*a*]pyrazine-3,8-dione derivatives **48-62** (see Scheme 1) because they were envisaged to possess affinity for the $hA_3$ AR subtype which was still of our interest, although being off-target for the work (see Results and Discussion for details).

## RESULTS AND DISCUSSION

### Chemistry

The new 8-amino-1,2,4-triazolo[4,3-*a*]pyrazin-3-one derivatives **1-15** and **16-26** were prepared as outlined in Schemes 1 and 2, respectively. The first set was synthesized starting from the ethyl 2-arylhydrazono-2-chloroacetates **27-30**,[23,33,34] prepared by reacting the suitable aryldiazonium chloride with ethyl 2-chloroacetoacetate, in the presence of sodium acetate in MeOH. Treatment of **27-30** with 33% aqueous ammonia in dioxane yielded the corresponding amino-derivatives **31-34**,[35,36] which were cyclized with triphosgene to yield the key intermediates ethyl 5-oxo-1-aryl-1H-1,2,4-triazole-3-carboxylates **35-38**.[37] Their $N^4$-alkylation with the suitable α-haloketones in DMF/$CH_3CN$, and in the presence of potassium carbonate, afforded the ethyl 1-aryl-5-oxo-1,2,4-triazole-3-carboxylate derivatives **39-47** whose cyclization with ammonium acetate, performed by conventional heating or under microwave irradiation, gave the 1,2,4-triazolo[4,3-*a*]pyrazine-3,8-dione derivatives **48-53**, **58-60**. The methoxy derivatives were demethylated with $BBr_3$ (**50-51**, **53** and **58**) or with 48% HBr in glacial acetic acid (**59**), to yield the corresponding hydroxy-substituted

compounds **54-56**, **61** and **62**. Catalytic (Pd/C) hydrogenation in a Parr apparatus of the 2-(4-nitrophenyl) derivative **52** furnished the 2-(4-aminophenyl) derivative **57**. The 3,8-diones **48-53**, **58-60** were chlorinated with phosphorus oxychloride, under microwave irradiation, to obtain the corresponding 8-chloro derivatives **63-71** which gave the desired 8-amino-1,2,4-triazolo[4,3-*a*]pyrazine-3-one derivatives **1-6**, **11-13** upon treatment with a saturated solution of ammonia in absolute ethanol. Demethylation of the methoxyphenyl derivatives **3**, **4**, **6**, **11** and **12** with $BBr_3$ gave the corresponding hydroxyphenyl-substituted compounds **7-9**, **14** and **15**. The 2-(4-nitrophenyl) derivative **5** was reduced ($H_2$, Pd/C) in a Parr apparatus to yield the corresponding 2-(4-aminophenyl) derivative **10**. The synthesis of compounds **16-27** is outlined in Scheme 2. Briefly, the derivatives were prepared by alkylation of the 6-(hydroxyphenyl) derivatives **14** or **15** with the suitable alkyl bromides, in refluxing 2-butanone and in the presence of potassium carbonate.

**Pharmacological Assays**

The 8-amino-2-aryl-1,2,4-triazolo[4,3-*a*]pyrazin-3-ones **1-26** and the 3,8-dione derivatives **48-62** were evaluated for their affinity to $hA_1$, $hA_{2A}$ and $hA_3$ ARs, stably transfected in Chinese hamster ovary (CHO) cells, and were also tested at the $hA_{2B}$ AR subtype by measuring their inhibitory effects on 5'-(N-ethyl-carboxamido)adenosine (NECA)-stimulated cAMP levels in $hA_{2B}$ CHO cells. Moreover, derivatives **12** and **20**, showing high $hA_{2A}$ AR affinity and selectivity, were studied by evaluating their effect on cAMP production in CHO cells, stably expressing $hA_{2A}$ AR, in order to assess the ability of these compounds to inhibit or stimulate the $A_{2A}$ AR. All pharmacological data are presented in Tables 1-2. The selected derivative **12** was also profiled for its protective effect against $MPP^+$-neurotoxicity in cultured human neuroblastoma SH-SY5Y cell lines, a widely used cellular PD model.[38,39] The results of these experiments are reported in Figures 1-3.

**Structure-affinity relationship studies**

The biological data reported in Tables 1-2 show that several new derivatives exhibited nanomolar affinity for $hA_1$, $hA_{2A}$ and $hA_3$ ARs thus indicating that the 1,2,4-triazolo[4,3-*a*]pyrazine-3-one is a valuable scaffold for developing new potent antagonists for these AR subtypes. All the tested compounds proved to be inactive ($IC_{50}$> 30000 nM) in inhibiting the NECA-stimulated cAMP levels in $hA_{2B}$ CHO cells. These results enabled us to deduce that compounds **1-29** and **48-62** lacked affinity for the $hA_{2B}$ AR. In fact, the $IC_{50}$ values obtained by our cAMP assays on reference ligands, such as 8-cyclopentyl-1,3-dipropyl-xanthine (DPCPX), NECA and 2-chloro-$N^6$–cyclopentyladenosine (CCPA) (Tables 1 and 2) well correlated with the $K_i$ values obtained from radioligand binding studies.[40,41]

*8-Amino-2-aryl-1,2,4-triazolo[4,3-a]pyrazin-3-one derivatives* **1-26**

As anticipated above, the main purpose of the work was to perform a preliminary investigation of the SARs of this new series and to identify new $hA_{2A}$ AR antagonists. This aim has been completely satisfied because four triazolopyrazines (**12**, **17**, **20** and **22**) possess high affinity ($K_i$= 2.9-10.6 nM) and a complete selectivity for the $hA_{2A}$ AR subtype. Several compounds (**2, 11, 14, 16**) show high affinity for the $hA_{2A}$ receptor ($K_i$ < 10 nM) and also bind to the $hA_1$ subtype with similar or just 5- to 6-fold reduced affinity. This behavior makes these derivatives interesting as well, because dual targeted antagonists of $hA_1$ and $hA_{2A}$ ARs have emerged as promising agents for the treatment of PD.[42-44] The $hA_1$ AR is presynaptically expressed on striatal dopaminergic neurons where it inhibits dopamine release.[45-46] Hence, dual $hA_1$ and $hA_{2A}$ AR antagonism would both facilitate dopamine release ($A_1$) and potentiate the post-synaptic response to dopamine ($A_{2A}$). Moreover, $hA_1$ ARs are also expressed in the hippocampus, neocortex and limbic system that are brain areas implicated in the control of cognitive and emotive functions.[1] Thus, $hA_1$ AR antagonists could ameliorate cognitive impairments associated with PD since they improve performance in an animal model of learning and memory.[43,44]

Some triazolopyrazines, possessing high affinity for both $hA_1$ and $hA_{2A}$ ARs, were also able to bind efficiently to the $hA_3$ AR subtype (**2**, **11**, **15**, **16**), the most active compound, being the 2,6-diphenyl derivative **2** ($K_i$= 11 nM).

Retracing the diverse phases of our work, we first synthesized a set of compounds (**1-4**, **7-8**) to evaluate which group, between methyl and phenyl, was the better for the 6-position. The 2,6-diphenyl-substituted derivative **2** turned out to be notable, showing high and comparable affinities for $hA_1$, $hA_{2A}$ and $hA_3$ ARs ($K_i$= 10-13 nM). The 6-methyl-2-phenyl derivative **1** was significantly less active, in particular for the targeted $hA_{2A}$ receptor. The para hydroxy substituent inserted on the 2-phenyl ring of **1** and **2**, was chosen because in the TQX series[28] it was profitable for $A_{2A}$ AR affinity. The 2-(4-hydroxyphenyl)-substituted **7** and **8** were less active at the $hA_{2A}$ AR than the unsubstituted derivatives **1** and **2** and also than the respective methoxy derivatives **3** and **4**, their synthetic precursors. The last two derivatives showed, on the whole, lower affinities for both $hA_1$ and $hA_{2A}$ ARs than their parent compounds **1** and **2**.

The comparison of AR affinities of the 6-methyl derivatives **1**, **3** and **7** with those of the corresponding 6-phenyl derivatives **2**, **4** and **8** highlighted that the 6-phenyl residue was more advantageous than the 6-methyl one, probably due to its higher lipophilicity and/or capability to enhance the structural complementarity of the whole molecule with the receptor binding site. Hence, subsequent investigations were carried out on the 6-phenyl-substituted compound **2** which was modified by introduction of a para amino group on the 2-phenyl residue (compound **10**), as suggested by affinity data of the TQX derivatives.[28] Compound **10** did not show enhanced affinity for the $hA_{2A}$ AR, with respect to the lead **2**, and the same applies to its synthetic precursor 2-(4-nitrophenyl) derivative **5**. On the contrary, $hA_1$ AR affinities of **5** and **10** were very high ($K_i$= 8.1 and 8.9 nM) and similar to that of **2**. The presence of a methoxy or hydroxy group at the ortho position of the 2-phenyl ring proved to be disadvantageous for the recognition of both $hA_{2A}$ and $hA_1$ ARs. In fact, compounds **6** and **9** are significantly less active than **2**, even if the $hA_{2A}$ affinity of the 2-(2-hydroxyphenyl) derivative **9** still remained good ($K_i$= 47 nM).

The binding data obtained within these first sets of compounds indicated that the best group for the 2-position was the unsubstituted phenyl ring. Thus, in the subsequent derivatives the 2-phenyl ring was maintained unmodified while structural changes were made at the 6-phenyl level. Introduction of a methoxy or hydroxy group at the meta (**11** and **14**) and para (**12** and **15**) positions on this moiety achieved interesting results, the most relevant being the identification of the 6-(4-methoxyphenyl) derivative **12** possessing nanomolar affinity ($K_i$= 7.2 nM) and a complete selectivity for the $hA_{2A}$ AR. Demethylation of compound **12** completely changed the affinity profile. The hydroxy derivative **15** shows, in fact, a 6-fold reduced $hA_{2A}$ AR affinity ($K_i$= 45 nM) and, above all, a nulled selectivity, being able to bind also $hA_1$ and $hA_3$ ARs with similar $K_i$ values. Moving the methoxy substituent from the para to the meta position (derivative **11**) maintained a high $hA_{2A}$ AR affinity ($K_i$= 6.8 nM) but lost selectivity, showing **11** to have considerable affinity also for the $hA_1$ AR and $hA_3$ ARs ($K_i$= 44 and 42 nM). Demethylation of compound **11** did not modify the affinity profile much, although compound **14** had a high affinity ligand for $hA_1$ and $hA_{2A}$ ARs ($K_i$= 14 and 3.5 nM, respectively) and quite a good one for $hA_3$ AR. Replacement of the 4-methoxy group with a methyl elicited a detrimental effect, which was difficult to explain, compound **13** being totally inactive.

In trying to enhance $hA_{2A}$ AR affinity or selectivity, we replaced the 3- and 4-methoxy group of **11** and **12** with propargyloxy (compounds **16** and **17**) and benzyloxy residues (derivatives **18** and **19**). These modifications were suggested by the SARs of different series of $hA_{2A}$ AR antagonists of similar size and shape, indicating that the presence of hindering substituents in suitable positions was often profitable for an effective and selective recognition of the $hA_{2A}$ AR.[3] Interestingly, affinities of the propargyloxy-derivatives **16** and **17** resemble those of the respective methoxy-substituted compounds **11** and **12**: both **16** and **17** showed nanomolar affinity for the $hA_{2A}$ AR ($K_i$= 5.1 and 10.6 nM) and **17** was also totally selective. On the contrary, the benzyloxy-derivatives **18** and **19** turned out to be significantly less active than **11** and **12**, in particular, the 3-benzyloxy derivative **18** was completely devoid of affinity for all the ARs. Given that the preferred position for

a substituent on the 6-phenyl ring seemed to be the para and that the steric bulk of the substituent seemed to play a key role in the binding, in the last step of the work, we modified derivative **12** by replacing the 4-methoxy group with other small alkoxy residues, containing either linear, unsaturated, branched or cyclic alkyl chains (compounds **20-26**). Within this new set of ligands, two other potent and completely selective $hA_{2A}$ AR antagonists were identified, i.e. the 4-ethoxyphenyl derivative **20** ($K_i$= 2.9 nM) and the 4-isopropoxyphenyl derivative **22** ($K_i$= 7.4 nM), bearing the smallest alkyl groups, among those evaluated. Instead, compounds **24** and **25**, bearing the cyclopropylmethoxy and cyclobutylmethoxy moieties, turned out to be inactive at the $hA_{2A}$ AR, as well as at the other ARs. For derivatives **23** and **26** no biological data are available since we met some difficulties in testing them, probably due to their scarce solubility in the assay medium. The same applies to **21** for the assays at the $hA_{2A}$ AR.

Finally, the selected derivatives **12** and **20**, showing high $hA_{2A}$ AR affinity and selectivity, were tested to evaluate their effect on cAMP production in CHO cells, stably expressing the $hA_{2A}$ AR. The obtained $IC_{50}$ values (Table 1) showed that **12** and **20** inhibited the NECA-induced increase of cAMP accumulation, thus behaving as antagonists.

*2-Aryl-1,2,4-triazolo[4,3-a]pyrazine-3,8-dione derivatives **48-62***

The triazolopyrazine-3,8-dione derivatives **48-62** were evaluated for their affinity for ARs since they were thought capable of binding the $hA_3$ AR subtype on the basis of overall nanomolar $hA_3$ AR affinities of the 1,4-dione derivatives of the TQX series.[26] Hence, since we were interested in identifying new $hA_3$ AR antagonists, although this was not the main purpose of this work, we decided to test the 3,8-dione derivatives **48-53**, **58-60** prepared as synthetic intermediates. Moreover, to further explore the SARs in this small set of derivatives, we synthesized compounds **54-56**, **57**, **61-62**. The obtained binding data (Table 2) partly confirmed our hypothesis. Although some derivatives showed null (**58-60**) or scarce affinity (**53**, **56**) for the $hA_3$ ARs, as for the other ARs, the remaining compounds displayed some affinities for the $hA_3$ AR subtype which are, on the

whole, higher. The most interesting was the 2-(4-hydroxyphenyl) derivative **55**, being a highly potent and selective ligand of the $hA_3$ AR ($K_i$= 0.37 nM). Also the 2-phenyl derivatives **48** ($R_6$= Me) and **49** ($R_6$= Ph) and the 2-(4-methoxyphenyl)-derivative **50** ($R_6$= Me) are worth noting showing good affinity ($K_i$= 60, 96 and 50 nM, respectively) and high selectivity for the $hA_3$ AR. Instead, the 2-(4-methoxyphenyl)- derivative **51** ($R_6$= Ph), even if selective, is less active as a $hA_3$ AR ligand ($K_i$= 214 nM). Demethylation of the 2-(4-methoxyphenyl) derivative **50,** as well as introduction of ortho-substituents (OMe, OH) on the 2-phenyl ring of **49**, significantly reduced the $hA_3$ AR affinity (see compounds **54**, and **53**, **56**, respectively). Good $hA_3$ AR binding activity ($K_i$= 63 nM) was displayed by the 2-(4-aminophenyl)- derivative **57** ($R_6$= Ph) which, however, is scarcely selective versus $hA_1$ and $hA_{2A}$ ARs. Insertion of OMe, Me, and OH substituents on the 6-phenyl moiety (compounds **58-62**) was detrimental to $hA_3$ AR affinity, with the exception of the 4-hydroxy group (compound **62**) which afforded a moderate affinity for this AR subtype ($K_i$= 207 nM).

It was not possible to test the 4-nitro derivative **52** at any of the ARs due to its scarce solubility in the assay medium. The same applies to the 4-hydroxy derivative **54** for the assays at the $hA_{2A}$ AR, since its low solubility did not allow it to reach high enough concentrations to obtain the dose-response curve.

**Neuroprotection studies in SH-SY5Y cell lines**

Parkinson's disease is the second most common neurodegenerative disorder of aging, characterized by motor bradykinesia, rigidity, resting tremor, and postural instability.[47] The progressive loss of dopaminergic neurons in the substantia nigra is the main cause of these deficits. Several mechanisms have been implicated as crucial to PD pathogenesis: oxidative stress, mitochondrial dysfunction, protein aggregation and misfolding, inflammation, excitotoxicity, apoptosis and other cell death pathways, and loss of trophic support. The aim of the current study was to examine the protective effects of the selected triazolopyrazine **12** on SH-SY5Y cells in an experimental *in*

*vitro* PD model. Several neurotoxins are employed to study neurodegeneration. In particular, $MPP^+$ is widely accepted as inducing neurotoxicity. The neurotoxin is able to induce dopaminergic toxicity through oxidation, hydrogen peroxide formation, and direct inhibition of the mitochondrial respiratory chain.[48] Much evidence indicates that SH-SY5Y cells possess many features of dopaminergic neurons and have been widely employed for the study of neuroprotection against PD-related neurotoxins. A pilot study was conducted to evaluate the neurotoxic effect produced by $MPP^+$ on SH-SY5Y cells. Cells were treated for 24 h with increasing doses of $MPP^+$ (50 μM to 3 mM). The results in Figure 1 show that $MPP^+$ produced a significant and concentration-dependent neurotoxic effect in this cell line. The dose of 1.5 mM, which caused 50% of cell death was chosen for the subsequent neuroprotection studies. Compound **12**, when administered alone, did not modify cell viability (Figure 2A) while at the concentration of 15 nM it was able to partially counteract MPP+-induced neurotoxicity (Figure 2B). In order to verify that the protective effect of **12** was due to the selective blockade of the $A_{2A}$ AR, we compared the effects of the compound with those of the well-known selective $hA_{2A}$ AR antagonist 4-(2-[7-amino-2-(2-furyl[1,2,4]-triazolo[2,3-*a*][1,3,5]triazin-5ylamino]ethyl)phenol **72** (ZM241385)[49] and we evaluated the effects of **12** in the presence of the selective $hA_{2A}$ AR agonist 2-[p-(2-carboxyethyl)phenethylamino]-5'-N-ethylcarboxamido adenosine **73** (CGS21680).[50] As shown in Figure 3A, the $hA_{2A}$ AR antagonist **72**, used at the concentration of 0.5 nM,[38] presented a neuroprotective effect on SH-SY5Y cells, thus counteracting $MPP^+$ toxicity. To validate the involvement of the $A_{2A}$ AR in the neuroprotective activity of **12** against $MPP^+$ toxicity, we evaluated the ability of the $hA_{2A}$ AR agonist **73** to reverse the effects of compound **12**. SH-SY5Y cells were treated with **12** (15 nM) in the presence of different **73** concentrations ranging from 10 to 100 nM. As shown in Figure 3B, the $hA_{2A}$ agonist **73** was able to suppress the protective effects of **12**, thus confirming that the effects of **12** may be attributed to the selective blockade of the $A_{2A}$ AR.

**Molecular modeling studies**

The binding mode of the synthesized compounds at the $hA_{2A}$ AR cavity was simulated with docking analysis by using the Molecular Operating Environment (MOE, 2014.09) docking tool and Gold and Autodock software.[51-54] The MOE software analysis was made by selecting the induced fit docking and optimization protocol (schematically, a preliminary docking analysis provides a set of ligand conformations that are energy minimized, including in this step the side chains of the receptor residues in proximity). For the docking tasks, two crystal structures of the $hA_{2A}$ AR in complex with the antagonist/inverse agonist **72** were employed (http://www.rcsb.org; pdb code: 3EML; 2.6-Å resolution and pdb code: 4EIY; 1.8-Å resolution[55-57]). The docking analysis was performed with different docking tools and two different crystal structures of the target to get an average prediction of the binding mode of the synthesized compounds at the binding cavity. For a subset of compounds, the binding modes at the $hA_1$ AR crystal structure (pdb code: 5UEN; 3.2-Å resolution)[58] and at a homology model of the $hA_3$ AR were also simulated with the same tools and protocols.

The docking results at the $hA_{2A}$ AR show that the molecules could bind to the pocket of this receptor with a preferred orientation ("type-one" conformations), presenting the substituent at the 2-position ($R_2$) located in the depth of the cavity and the $R_6$ group at the entrance of the binding site (Figure 4A). The scaffold adopts a position that makes it able to interact with Asn253$^{6.55}$ and Glu169 (EL2) through H-bond contacts, while a π-π interaction is present between the phenyl ring of Phe168 (EL2) and the bicyclic core of the compounds (Figure 4B). This interaction is very similar to the one given by the co-crystallized compound **72**[55,57] and by other structural classes of $hA_{2A}$ AR ligands previously described.[22,23]

A second binding mode ("type-two" conformations) simulated by docking experiments presents the scaffold oriented in the opposite way with respect to the conformations described above, the 6-substituent being located in the depth of the cavity and the 2-substituent pointing toward the extracellular environment. This second binding mode is generally not preferred at the $hA_{2A}$ AR,

being associated with lower docking scores than those of the above described docking conformations, except for derivatives presenting ortho-substituent on the 2-phenyl ring (see below). Compound **2** can be considered the reference ligand of the series, as it bears two unsubstituted phenyl rings at the 2- and 6- positions. This derivative showed good affinity at the $hA_1$ AR, $hA_{2A}$ AR and $hA_3$ AR and this makes it a sort of passe-partout for the three ARs. Docking results of compound **2** at the three AR structures showed that it may be inserted in the receptor cavities with the two binding modes, both associated with good docking scores (the "type-one" generally preferred). The possibility of making more than one complex with the same receptor could result in good affinity and this feature could be applied at the three ARs.

The substituents inserted on the 2-phenyl group modulate the interaction with the binding pocket. In detail, the presence of small groups at the para-position generally affords decreased $hA_{2A}$ AR affinity, with respect to the corresponding analogues with an unsubstituted 2-phenyl ring (compare derivatives **3** and **7** with **1** and compounds **4**, **5**, **8**, and **10** with **2**). This result was interpreted considering various parameters. The first is the topological complementarity of the ligand with the binding pocket (Figure 4C). The presence of a para-substituent on the 2-phenyl ring seems to cause a slight displacement of the ligand that decreases its ability in establishing some crucial interactions with the receptor (i.e. H-bonds with $Asn253^{6.55}$ and Glu169) with respect to the compounds with an unsubstituted 2-phenyl ring.

Secondly, $hA_{2A}$ AR affinities may be rationalized by docking results also considering that the depth of the binding cavity is mainly hydrophobic. Hence, a non-polar group at the para-position of the 2-phenyl ring, such as the methoxy group of **4** ($K_i$= 78 nM), would afford a slightly better interaction with the target, when compared to a more polar group at the same position, such as the OH group of **8** ($K_i$= 138 nM). In this sense, we compared logP and $pK_i$ values of compounds bearing an unsubstituted 2-phenyl ring (**1** and **2**) with those of the corresponding derivatives presenting para-substituents on this ring. We observed a well-conserved trend of logP and $pK_i$ values for the two groups of ligands (compare derivatives **3** and **7** to **1** and derivatives **4**, **5**, **8**, **10** to **2**, Figure 5A-B).

On this basis, we conclude that a para-substituent on the 2-phenyl ring is fairly allowed for these compounds and, if present, should be a small hydrophobic function.

To evaluate the interaction of compounds bearing a 2-phenyl (derivative **2**) and a 2-para-substituted-phenyl moiety (compounds **4**, **5**, **8**, and **10**) with the receptor residues, in proximity of the 2-substituent, we also employed the *IF-E 6.0* tool (see Experimental section for details) that calculates the atomic and residue interaction forces and the per-residue interaction energies (expressed as kcal x $mol^{-1}$). This tool has been previously used for analogue analyses at hARs.[59-61] The results are graphically displayed in Figure 5C-D and indicate that a higher ligand-target interaction is observed when the 2-phenyl ring is unsubstituted (**2**) or presents a non-polar para-substituent (**4**). Polar or electron-rich para-substituents, such as nitro (**5**), hydroxyl (**8**), or amino (**10**), provide some interaction only with polar receptor residues, such as His250$^{6.52}$. These results are in good agreement with the affinity data at the $hA_{2A}$ AR for the analyzed compounds.

Interestingly, several derivatives featuring polar para-substituents on the 2-phenyl ring (**5**, **8** and **10**) are endowed with high affinity for the $hA_1$ AR, compounds **5** and **10** being the most active. Docking results showed that these ligands present both the binding modes at the $hA_1$ AR with corresponding good scores. The "type two" binding mode at the $hA_1$ AR is favoured by polar interactions with Asn70$^{2.65}$, Glu170 (EL2), Ser267 (EL3) and Tyr271$^{7.36}$. While the last residue is conserved among ARs, the others, i.e. Asn70$^{2.65}$, Glu170 and Ser267, are specific of the $hA_1$ AR, being substituted by a serine and two leucines in the $hA_{2A}$ AR (Ser67$^{2.65}$, Leu167 and Leu267) and by a serine and two glutamines in the $hA_3$ AR (Ser73$^{2.65}$, Gln167 and Gln261). The possibility of giving two good score binding modes at the $hA_1$ AR, not observed at $hA_{2A}$ and $hA_3$ ARs, could help to explain the $hA_1$ AR affinity and selectivity of compounds **5**, **8** and **10**. The "type-two" docking conformation of compound **10** at the $hA_1$ AR is reported in the Supporting information (Figure S1).

Introduction of a substituent (OMe, OH) at the ortho-position of the 2-phenyl ring of compound **2** afforded derivatives **6** and **9**, endowed with 20- to 30-fold reduced $hA_{2A}$ AR affinity. When **6** and **9** are inserted into the binding site with the 2-aryl located in the depth of the cavity, the ortho-

substituent may be oriented toward the 3-carbonyl group or the N-1 scaffold atom. In the first case, the ortho-hydroxy substituent (derivative **9**) makes an internal H-bond interaction with the carbonyl group but this leads to a reorientation of the 2-phenyl ring with respect to the bicyclic scaffold plane. The presence of the ortho-methoxy substituent (derivative **6**) makes the reorientation of the 2-phenyl ring even more evident due to the repelling effect between the ortho-methoxy and the 3-carbonyl function. Consequently, these docking conformations are associated with a low docking score for all the employed software. When the ortho-substituent is oriented toward the N-1 atom, the reorientation of the 2-phenyl ring, with respect to the bicyclic core, is greatly reduced, but the ligands get displaced with respect to compound **2**, due to the steric clash with Asn253$^{6.55}$ (even if a polar interaction might occur between the ortho-substituent and the Asn253$^{6.55}$ side chain). Even these docking conformations appear associated with a low score. Docking results suggest that compounds **6** and **9** preferentially adopt the "type-two" orientation with the 2-aryl pendant located at the entrance of the cavity and the $R_6$ group positioned in the depth of the pocket (Figure 6A). In this way, the ortho-hydroxy group of derivative **9** could give some polar interaction with Glu169 (EL2). An analogue arrangement was observed at the $hA_1$ AR, where the ortho-hydroxy group of **9** could interact with Glu172 (corresponding to Glu169 of the $hA_{2A}$ AR) and also with Glu170 (corresponding to Leu167 of the $hA_{2A}$ AR). This binding mode could give some interpretation of the slight $hA_1$ AR selectivity of compound **9**.

Docking results of compounds bearing an unsubstituted 2-phenyl ring and various aryl substituents at the $R_6$ position (**11-26**) again show a preferential binding mode with the 2-group located in the depths of the cavity and the 6-substituent pointing toward the external environment. Hence, the substituents on the 6-phenyl ring are generally located at the entrance of the cavity, providing different degrees of interaction with the receptor residues in proximity. Considering the effects of substituents at the para-position of the 6-phenyl ring, the introduction of a polar hydroxyl group led to a decrease in $hA_{2A}$ AR affinity (**15**, $K_i$= 45 nM) with respect to the unsubstituted analogue **2**. Docking results suggest that this hydroxy group is inserted within a set of hydrophobic amino acid

residues, such as Leu167 (EL2), Leu267 (EL3) and Tyr271$^{7.36}$, thus helping to explain the non-optimal interaction of the 6-(4-phenol) group (**15**) with the receptor site, with respect to the phenyl ring (**2**). On the same basis, we may interpret why the introduction of non-polar groups at the para-position of the 6-phenyl ring is generally well tolerated, leading to compounds (**12**, **17**, **20**, and **22**) with similar affinity with respect to the corresponding analogue **2**, lacking a substituent on the 6-phenyl ring. Figure 6B shows the binding mode of compound **20** with a focus on the residues located in proximity of the $R_6$ substituent. The para-ethoxy substituent of **20** appears inserted among the above cited hydrophobic residues Leu167 (EL2), Leu267 (EL3), and Tyr271$^{7.36}$. Insertion of a phenyl ring on the methoxy group of **12**, to give compound **19**, lowered the $hA_{2A}$ AR affinity even if it was still in the high nanomolar range ($K_i$= 708 nM). Interestingly, compounds **24** and **25** bearing a smaller moiety at the same position, such as cyclopropylmethoxy and a cyclobutyloxy group, respectively, completely lack binding activity, not only at the $hA_{2A}$ AR but also at the other hARs. Docking results show that the benzyloxy substituent of **19** is partially exposed to the external environment, in a position that makes it able to give π-π interaction with Tyr271$^{7.36}$ and also to interact with the polar hydrogen atoms of Lys153 (EL2) and Tyr271$^{7.36}$ side chains. Hence, this docking pose could justify both the decreased affinity, considering the exposure of the phenyl group to the solvent, and the maintenance of at least high nanomolar binding.

In the case of compounds **24** and **25**, the cycloalkyl groups are in a comparable position to that of the external phenyl group of **19**. They are exposed to the solvent but they are not able, as the benzyl, to provide the above cited interactions with the receptor residues. This could help to interpret the lower affinity of these two compounds. Nevertheless, modeling results do not clearly depict the loss of affinity of these compounds with respect to other analogues presenting slightly smaller alkyl groups and very high affinity (such as compound **22**, $K_i$= 7.45 nM).

Considering the docking results at the $hA_1$ AR, it has to be noted that in this AR subtype the above cited Leu167 (EL2), Leu267 (EL3), and Tyr271$^{7.36}$ of the $hA_{2A}$ AR are replaced by Glu170 (EL2), Ser267 (EL3), and Tyr271$^{7.36}$. As a consequence, the presence of hydrophobic substituents at the

para-position of the 6-phenyl ring was less tolerated by the $hA_1$ AR, with respect to the $hA_{2A}$ AR, thus justifying the low to null $hA_1$AR affinity of compounds **16-26**.

In the case of derivatives with substituents at the meta-position of the 6-phenyl ring, the affinity data show that the nature of the substituent does not significantly influence the receptor-ligand interaction, since the presence of a polar hydroxyl group (**14**) or non-polar functions, such as methoxy or propargyloxy groups (**11**, and **16**, respectively) leads to analogue affinities at the $hA_{2A}$ AR. Figure 6B shows the presence on the receptor of non-polar groups (i.e. the alkyl chain of Ile66$^{2.64}$) as well as polar functions (i.e. the carbonyl groups of Ile66$^{2.64}$ and Ser67$^{2.65}$) in proximity with the meta-position of the 6-phenyl ring. On the other hand, while the introduction of a benzyloxy group at the para-position of the 6-phenyl ring of **2**, to obtain **19**, was fairly tolerated, although causing a significant decrease of $hA_{2A}$ AR affinity, the introduction of the same group at the meta-position led to an inactive compound (**18**). This chain may be oriented toward either the trans-membrane (TM) domains or the extracellular environment. In the first case, there would be a clash with the TM atoms, while in the second case the hydrophobic benzyloxy chain would be completely exposed to the solvent without interacting significantly with receptor residues. Similar considerations can be made for the $hA_1$ AR, where the presence of polar residues at the entrance of the receptor cavity (see above) makes hydrophobic substituents at the meta-position of the 6-phenyl ring less beneficial for the $hA_1$ AR binding than for the $hA_{2A}$ receptor-ligand interaction.

## CONCLUSION

This work has led to the identification of the 1,2,4-triazolo[4,3-*a*]pyrazin-3-one as a new versatile scaffold for the development of hAR antagonists. In fact, several synthesized compounds are endowed with nanomolar affinities and have different degrees of selectivity for $hA_1$, $hA_{2A}$ and $hA_3$ AR subtypes. Very interestingly, some 8-amino-2-phenyl-1,2,4-triazolopyrazin-3-one derivatives, featuring small para-alkoxy substituents on the 6-phenyl ring, show high affinity ($K_i$= 2.9-10.6 nM) and a complete selectivity for the targeted $hA_{2A}$ AR subtype. The potent and selective $hA_{2A}$ AR

antagonist **12** is able to partially counteract $MPP^+$-induced neurotoxicity in cultured human neuroblastoma SH-SY5Y cells, a widely used cellular PD model. The results of the docking studies at hAR structures permit us to explain some of the observed affinity data in terms of ligand-receptor molecular interactions, and provide useful indications for the design of new 8-amino-triazolo[4,3-*a*]pyrazin-3-one derivatives as $hA_{2A}$ AR antagonists.

## EXPERIMENTAL PROCEDURES

**Chemistry**. The microwave-assisted syntheses were performed using an Initiator EXP Microwave Biotage instrument (frequency of irradiation: 2.45 GHz). Analytical silica gel plates (Merck F254) and silica gel 60 (Merck, 70-230 mesh) were used for analytical TLC and for column chromatography, respectively. All melting points were determined on a Gallenkamp melting point apparatus and are uncorrected. Elemental analyses were performed with a Flash E1112 Thermofinnigan elemental analyzer for C, H, N and the results were within ± 0.4% of the theoretical values. All final compounds revealed purity not less than 95%. The IR spectra were recorded with a Perkin-Elmer Spectrum RX I spectrometer in Nujol mulls and are expressed in $cm^{-1}$. NMR spectra were recorded on a Bruker Avance 400 spectrometer (400 MHz). The chemical shifts are reported in δ (ppm) and are relative to the central peak of the residual nondeuterated solvent, which was $CDCl_3$ or $DMSOd_6$. The following abbreviations are used: s= singlet, d= doublet, t= triplet, q= quartet, m= multiplet, br= broad and ar= aromatic protons.

**General Procedure for the Synthesis of 8-Amino-2-aryl-1,2,4-triazolo[4,3-*a*]pyrazin-3(2*H*)-one derivatives (1-6).**

A suspension of the 8-chloro-triazolopyrazine derivatives **63-71** (1 mmol) in a saturated solution of $NH_3$ in absolute ethanol (30 mL) was heated at 120 °C in a sealed tube for 16 h. The mixture was

cooled at room temperature and the solid was collected by filtration, washed with water (about 5-10 mL), dried and recrystallized.

*8-Amino-6-methyl-2-phenyl-1,2,4-triazolo[4,3-a]pyrazin-3(2H)-one (**1**).* Yield 92%; mp 258-259 °C (Toluene). $^1$H NMR (DMSO-$d_6$) 2.11 (s, 3H, $CH_3$), 7.09 (s, 1H, H-5), 7.35 (t, 1H, ar, J = 6.6 Hz), 7.40 (br s, 2H, $NH_2$), 7.54 (t, 2H, ar, J = 7.7 Hz), 8.05 (d, 2H, ar, J = 7.7 Hz). Anal. Calc. for $C_{12}H_{11}N_5O$.

*8-Amino-2,6-diphenyl-1,2,4-triazolo[4,3-a]pyrazin-3(2H)-one (**2**).* Yield 50%; mp 276-277 °C ($CH_3NO_2$). $^1$H NMR (DMSO-$d_6$) 7.33-7.38 (m, 2H, ar), 7.43 (t, 2H, ar, J = 7.4 Hz), 7.55-7.59 (m, 4H, 2 ar + $NH_2$), 7.77 (s, 1H, H-5), 7.98 (d, 2H, ar, J = 7.5 Hz), 8.08 (d, 2H, ar, J = 7.9 Hz). Anal. Calc. for $C_{17}H_{13}N_5O$.

*8-Amino-6-methyl-2-(4-methoxyphenyl)-1,2,4-triazolo[4,3-a]pyrazin-3(2H)-one (**3**).* Yield 83%; mp 243-244 °C (EtOH/2-Methoxyethanol). $^1$H NMR (DMSO-$d_6$) 2.11 (s, 3H, $CH_3$), 3.81 (s, 3H, $OCH_3$), 7.07 (s, 1H, H-5), 7.09 (d, 2H, ar, J = 9.1 Hz), 7.36 (br s, 2H, $NH_2$), 7.90 (d, 2H, ar, J = 9.1 Hz). Anal. Calc. for $C_{13}H_{13}N_5O_2$.

*8-Amino-2-(4-methoxyphenyl)-6-phenyl-1,2,4-triazolo[4,3-a]pyrazin-3(2H)-one (**4**).* Yield 84 %; mp 254-255 °C ($CH_3NO_2$). $^1$H NMR (DMSO-$d_6$) 3.82 (s, 3H, $OCH_3$), 7.13 (d, 2H, ar, J = 8.8 Hz), 7.33-7.45 (m, 3H, ar), 7.56 (br s, 2H, $NH_2$), 7.75 (s, 1H, H-5), 7.92-7.99 (m, 4H, ar). IR 3366, 3311, 1644. Anal. Calc. for $C_{18}H_{15}N_5O_2$.

*8-Amino-2-(4-nitrophenyl)-6-phenyl-1,2,4-triazolo[4,3-a]pyrazin-3(2H)-one (**5**).* Yield 62%; mp 290-291 °C (Cyclohexane/EtOAc). $^1$H NMR (DMSO-$d_6$) 7.13 (t, 1H, ar, J = 8.8 Hz), 7.35 (t, 2H, ar, J = 7.5 Hz), 7.69 (br s, 2H, $NH_2$), 7.79 (s, 1H, H-5), 7.99 (d, 2H, ar, J = 7.5 Hz), 8.38 (d, 2H, ar, J = 9.3 Hz), 8.48 (d, 2H, ar, J = 9.3 Hz). IR 3366, 3311, 1644. Anal. Calc. for $C_{17}H_{12}N_6O_3$.

*8-Amino-2-(2-methoxyphenyl)-6-phenyl-1,2,4-triazolo[4,3-a]pyrazin-3(2H)-one (**6**).* Yield 74 %; mp 257-258 °C ($CH_3NO_2$). $^1$H NMR (DMSO-$d_6$) 3.80 (s, 3H, $OCH_3$), 7.11 (t, 1H, ar, J= 7.6 Hz), 7.26 (d, 1H, ar, J = 8.3 Hz), 7.35 (t, 1H, ar, J = 7.3 Hz), 7.43 (t, 2H, ar, J = 7.3 Hz), 7.49-7.56 (m, 4H, 2ar + $NH_2$), 7.73 (s, 1H, H-5), 7.97 (d, 2H, ar, J = 7.5 Hz). Anal. Calc. for $C_{18}H_{15}N_5O_2$.

**General Procedure for the Synthesis of 2-(Hydroxyphenyl)-substituted 8-amino-2-phenyl-1,2,4-triazolo[4,3-*a*]pyrazin-3(2*H*)-one (7-9).**

1 M solution of $BBr_3$ in dichloromethane (5.1 mL) was slowly added at 0 °C, under nitrogen atmosphere, to a suspension of the methoxy-substituted triazolopyrazines **3**, **4**, **6** (1.02 mmol) in anhydrous dichloromethane (20 mL). The mixture was stirred at rt until the disappearance of the starting material (TLC monitoring, 5-16 h), then was diluted with water (10 mL) and neutralized with a $NaHCO_3$ saturated solution. The organic solvent was removed by evaporation at reduced pressure and the solid was collected by filtration. The crude derivatives were dried and purified by recrystallization.

*8-Amino-2-(4-hydroxyphenyl)-6-methyl-1,2,4-triazolo[4,3-a]pyrazin-3(2H)-one (**7**).* Yield 65%; mp > 300 °C (EtOH/2-Methoxyethanol). $^1$H NMR (DMSO-$d_6$) 2.11 (s, 3H, $CH_3$), 6.88 (d, 2H, ar, J = 6.8 Hz), 7.06 (s, 1H, H-5), 7.33 (br s, 2H, $NH_2$), 7.75 (d, 2H, ar, J = 6.8 Hz). 9.69 (br s, 1H, OH). Anal. Calc. for $C_{12}H_{11}N_5O_2$.

*8-Amino-2-(4-hydroxyphenyl)-6-phenyl-1,2,4-triazolo[4,3-a]pyrazin-3(2H)-one (**8**).* Yield 72%; mp > 300 °C (EtOH). $^1$H NMR (DMSO-$d_6$) 6.91 (d, 2H, ar, J = 8.5 Hz), 7.34 (t, 1H, ar, J = 7.5 Hz), 7.43 (t, 2H, ar, J = 7.5 Hz), 7.53 (br s, 2H, $NH_2$), 7.74 (s, 1H, H-5), 7.78 (d, 2H, ar, J = 8.5 Hz), 7.97 (d, 2H, ar, J = 7.8 Hz), 9.72 (s, 1H, OH). IR 3393-3122, 1642, 1667. Anal. Calc. for $C_{17}H_{13}N_5O_2$.

*8-Amino-2-(2-hydroxyphenyl)-6-phenyl-1,2,4-triazolo[4,3-a]pyrazin-3(2H)-one (**9**).* Yield 67%; mp 271-273 °C (2-Methoxyethanol). $^1$H NMR (DMSO-$d_6$) 6.95 (t, 1H, ar, J = 7.5 Hz), 7.03 (d, 1H, ar, J = 8.1 Hz), 7.33-7.44 (m, 5H, ar), 7.55 (br s, 2H, $NH_2$), 7.75 (s, 1H, H-5), 7.98 (d, 2H, ar, J = 7.5 Hz), 9.88 (s, 1H, OH). Anal. Calc. for $C_{17}H_{13}N_5O_2$.

**8-Amino-2-(4-aminophenyl)-6-phenyl-1,2,4-triazolo[4,3-*a*]pyrazin-3-(2*H*)one (10).**

10 % Pd/C (20% w/w with respect to the nitro derivative) was added to a solution of the 2-(4-nitrophenyl) derivative **5** (0.8 mmol) in DMF (4 mL). The mixture was hydrogenated in a Parr

apparatus at 45 psi for 24 h. Then the catalyst was filtered off and the clear solution was diluted with water (about 50 mL) to obtain a solid that was collected by filtration, washed with water and $Et_2O$, dried and recrystallized. Yield 39 %; mp >300 °C (2-Methoxyethanol). $^1$H NMR (DMSO-$d_6$) 5.33 (br s, 2H, $NH_2$), 6.68 (d, 2H, ar, J = 8.7 Hz), 7.34 (t, 1H, ar, J = 7.2 Hz), 7.42 (t, 2H, J = 7.4 Hz), 7.49 (br s, 2H, $NH_2$), 7.57 (d, 2H, J = 8.7 Hz), 7.72 (s, 1H, H-5), 7.96 (d, 2H, ar, J = 7.4 Hz). Anal. Calc. for. $C_{17}H_{14}N_6O$.

**General Procedure for the Synthesis of 8-Amino-2-aryl-1,2,4-triazolo[4,3-*a*]pyrazin-3(2*H*)-one derivatives (11-13).**

The tile compounds were obtained by reacting the 8-chloro-triazolopyrazine derivatives **69-71** (1 mmol) in the same experimental conditions as described above to prepare **1-6**. The crude derivatives were purified by recrystallization.

*8-Amino-6-(3-methoxyphenyl)-2-phenyl-1,2,4-triazolo[4,3-a]pyrazin-3(2H)-one (**11**).* Yield 66%; mp 249-251 °C (EtOH). $^1$H NMR (DMSO-$d_6$) 3.83 (s, 3H, $OCH_3$), 6.90-6.93 (m, 1H, ar), 7.31-7.37 (m, 2H, ar), 7.53-7.58 (m, 6H, 4 ar + $NH_2$), 7.81 (s, 1H, H-5), 8.07 (d, 2H, ar, J = 7.5 Hz). IR 3358, 3312, 1703, 1645. Anal. Calc. for $C_{18}H_{15}N_5O_2$.

*8-Amino-6-(4-methoxyphenyl)-2-phenyl-1,2,4-triazolo[4,3-a]pyrazin-3(2H)-one (**12**).* Yield 94%; mp 251-252 °C (EtOH/2-Methoxyethanol). $^1$H NMR (DMSO-$d_6$) 3.80 (s, 3H, $OCH_3$), 6.99 (d, 2H, ar, J = 8.7 Hz), 7.36 (t, 1H, ar, J = 7.5 Hz), 7.54-7.58 (m, 4H, 2ar + $NH_2$), 7.67 (s, 1H, H ), 7.92 (d, 2H, ar, J = 8.7 Hz), 8.08 (d, 2H, ar, J = 8.5 Hz). IR 3381, 3308, 1697, 1649. Anal. Calc. for $C_{18}H_{15}N_5O_2$.

*8-Amino-6-(4-methylphenyl)-2-phenyl-1,2,4-triazolo[4,3-a]pyrazin-3(2H)-one (**13**).* Yield 75%; mp 287-288 °C (2-Methoxyethanol). $^1$H NMR (DMSO-$d_6$) 2.34 (s, 3H, $CH_3$), 7.24 (d, 2H, ar, J = 7.9 Hz), 7.36 (t, 1H, ar, J = 7.4 Hz), 7.54-7.58 (m, 4H, 2 ar + $NH_2$), 7.70 (s, 1H, H-5), 7.87 (d, 2H, ar, J = 7.9 Hz), 8.07 (d, 2H, ar, J = 7.6 Hz). IR 3366, 3310, 1701, 1651. Anal. Calc. for $C_{18}H_{15}N_5O$.

**General Procedure for the Synthesis of 6-(Hydroxyphenyl)-substituted 8-amino-2-phenyl-1,2,4-triazolo[4,3-*a*]pyrazin-3(2*H*)-one (14, 15).**

The tile compounds were obtained by reacting the corresponding methoxy derivatives **11, 12** (1.02 mmol) with $BBr_3$ in the same experimental conditions as described above to prepare compounds **7-9**. The crude derivatives were dried and purified by recrystallization.

*8-Amino-6-(3-hydroxyphenyl)-2-phenyl-1,2,4-triazolo[4,3-a]pyrazin-3(2H)-one (**14**).* Yield 93%; mp >300 °C (EtOH/2-Methoxyethanol). $^1$H NMR (DMSO-$d_6$) 6.75 (d, 1H, ar J = 7.3 Hz), 7.21 (t, 1H, ar, J = 7.4 Hz), 7.36-7.38 (m, 3H, ar), 7.55-7.61 (m, 4H, 2 ar + $NH_2$), 7.61 (s, 1H, H-5), 8.08 (d, 2H, ar, J = 8.1 Hz), 9.45 (s, 1H, OH). Anal. Calc. for $C_{17}H_{13}N_5O_2$.

*8-Amino-6-(4-hydroxyphenyl)-2-phenyl-1,2,4-triazolo[4,3-a]pyrazin-3(2H)-one (**15**).* Yield 85%; mp 285-286 °C (EtOH/2-Methoxyethanol). $^1$H NMR (DMSO-$d_6$) 6.81 (d, 2H, ar, J = 6.8 Hz), 7.35 (t, 1H, ar, J = 7.4 Hz), 7.40 (t, 2H, ar, J = 7.6 Hz), 7.53 (br s, 2H, $NH_2$), 7.73 (s, 1H, H-5), 7.79 (d, 2H, ar, J = 6.8 Hz), 8.08 (d, 2H, ar, J = 7.6 Hz), 9.58 (s, 1H, OH). IR 3379-3294, 1694, 1643 $cm^{-1}$. Anal. Calc. for $C_{17}H_{13}N_5O_2$.

**General Procedure for the Synthesis of 8-Amino-6-(alkyloxyphenyl)-2-phenyl-1,2,4-triazolo[4,3-*a*]pyrazin-3(2*H*)-ones (16-26).**

A solution of the suitable alkyl bromide (1.2 mmol) in butan-2-one (3 mL) was added dropwise to a mixture of the hydroxyphenyl- derivative **14** or **15** (1 mmol) and $K_2CO_3$ (2 mmol) in butan-2-one (5 mL). The mixture was heated at reflux until the disappearance of the starting hydroxy-derivative (TLC monitoring, 7-58 h). After cooling at room temperature, the solid was collected by filtration, washed with water, dried and recrystallized.

*8-Amino-2-phenyl-6-(3-propargyloxyphenyl)-1,2,4-triazolo[4,3-a]pyrazin-3(2H)-one (**16**).* Yield 58%; mp 217-219 °C (EtOH/2-Methoxyethanol). $^1$H NMR (DMSO-$d_6$) 3.58 (t, 1H, CH, J = 2.3 Hz), 4.89 (d, 2H, $CH_2$, J = 2.3 Hz), 6.97 (d, 1H, ar, J = 6.5 Hz), 7.36 (t, 2H, ar, J = 7.6 Hz), 7.55-

7.63 (m, 6H, 4ar + $NH_2$), 7.84 (s, 1H, H-5), 8.08 (d, 2H, ar, J = 7.6 Hz). IR 3443, 3298, 1721, 1643 $cm^{-1}$. Anal. Calc. for $C_{20}H_{15}N_5O_2$.

*8-Amino-2-phenyl-6-(4-propargyloxy)phenyl-1,2,4-triazolo[4,3-a]pyrazin-3(2H)-one* ***(17)***. Yield 56%; mp 244-245 °C (AcOH). $^1$H NMR (DMSO-$d_6$) 3.59 (t, 1H, CH, J = 2.3 Hz), 4.85 (d, 2H, $CH_2$, J = 2.4 Hz), 7.04 (d, 2H, ar, J = 6.9 Hz), 7.36 (t, 1H, ar, J = 7.4 Hz), 7.54-7.59 (m, 4H, 2ar + $NH_2$), 7.69 (s, 1H, H-5), 7.93 (d, 2H, ar, J = 6.9 Hz), 8.08 (d, 2H, ar, J = 7.6 Hz). IR 3458, 3331, 3219, 1695, 1620. Anal. Calc. for $C_{20}H_{15}N_5O_2$.

*8-Amino-6-(3-benzyloxyphenyl)-2-phenyl-1,2,4-triazolo[4,3-a]pyrazin-3(2H)-one* ***(18)***. Yield 78%; mp 264-266 °C (2-Methoxyethanol). $^1$H NMR (DMSO-$d_6$) 5.19 (s, 2H, $CH_2$), 6.99 (d, 1H, ar, J = 8.3 Hz), 7.32-7.65 (m, 13H, 11ar + $NH_2$), 7.84 (s, 1H, H-5), 8.07 (d, 2H, ar, J = 8.0 Hz). Anal. Calc. for $C_{24}H_{19}N_5O_2$.

*8-Amino-6-(4-benzyloxyphenyl)-2-phenyl-1,2,4-triazolo[4,3-a]pyrazin-3(2H)-one* ***(19)***. Yield 78%; mp 284-285 °C (2-Methoxyethanol). $^1$H NMR (DMSO-$d_6$) 5.16 (s, 2H, $CH_2$), 7.07 (d, 2H, ar, J = 8.9 Hz), 7.34-7.48 (m, 6H, ar), 7.51-7.58 (m, 4H, 2ar + $NH_2$), 7.67 (s, 1H, H-5), 7.92 (d, 2H, ar, J = 8.9 Hz), 8.08 (d, 2H, ar, J = 7.6 Hz). IR 3362, 3310, 1697, 1647. Anal. Calc. for $C_{24}H_{19}N_5O_2$.

*8-Amino-6-(4-ethoxyphenyl)-2-phenyl-1,2,4-triazolo[4,3-a]pyrazin-3(2H)-one* ***(20)***. Yield 72%; mp 267-268 °C (EtOH/2-Methoxyethanol). $^1$H NMR (DMSO-$d_6$) 1.35 (t, 3H, $CH_3$, J = 7.0 Hz), 4.07 (q, 2H, $CH_2$, J = 7.0 Hz), 6.96 (d, 2H, ar, J = 6.8 Hz), 7.36 (t, 1H, ar, J = 8.8 Hz), 7.53-7.58 (m, 4H, 2ar + $NH_2$), 7.65 (s, 1H, H-5), 7.90 (d, 2H, ar, J = 6.8 Hz), 8.08 (d, 2H, ar, J = 8.8 Hz). IR 3119, 3102, 1697, 1647. Anal. Calc. for $C_{19}H_{17}N_5O_2$.

*8-Amino-6-(4-n-propyloxyphenyl)-2-phenyl-1,2,4-triazolo[4,3-a]pyrazin-3(2H)-one* ***(21)***. Yield 67%; mp 266-267 °C (2-Methoxyethanol). $^1$H NMR (DMSO-$d_6$) 0.99 (t, 3H, $CH_3$, J = 7.4 Hz), 1.72-1.77 (m, 2H, $CH_2$), 3.97 (t, 2H, $CH_2$, J = 6.5 Hz), 6.97 (d, 2H, ar, J = 8.8 Hz), 7.35 (t, 1H, ar, J = 7.3 Hz), 7.54-7.58 (m, 4H, 2ar + $NH_2$), 7.65 (s, 1H, H-5), 7.89 (d, 2H, ar, J = 8.8 Hz), 8.07 (d, 2H, ar, J = 7.9 Hz). Anal. Calc. for $C_{20}H_{19}N_5O_2$.

*8-Amino-6-(4-isopropyloxyphenyl)-2-phenyl-1,2,4-triazolo[4,3-a]pyrazin-3(2H)-one* ***(22)***. Yield 70%; mp 240-241 °C (EtOH/2-Methoxyethanol). $^1$H NMR (DMSO-$d_6$) 1.30 (d, 6H, 2$CH_3$, J = 6.0 Hz), 4.63-4.69 (m, 1H, CH), 6.96 (d, 2H, ar, J = 8.7 Hz), 7.36 (t, 1H, ar, J = 7.4 Hz), 7.52 (br s, 2H, $NH_2$), 7.58 (m, 2H, ar, J = 7.7 Hz), 7.64 (s, 1H, H-5), 7.88 (d, 2H, ar, J = 8.7 Hz), 8.08 (d, 2H, ar, J = 7.9 Hz). IR 3385, 3310, 1701, 1638. Anal. Calc. for $C_{20}H_{19}N_5O_2$.

*8-Amino-6-(4-isobutyloxyphenyl)-2-phenyl-1,2,4-triazolo[4,3-a]pyrazin-3(2H)-one* ***(23)***. Yield 64%; mp 249-251 °C (2-Methoxyethanol). $^1$H NMR (DMSO-$d_6$) 1.00 (d, 6H, 2$CH_3$, J= 6.5 Hz), 1.99-2.06 (m, 1H, CH), 3.78 (d, 2H, $CH_2$, J = 6.5 Hz), 6.97 (d, 2H, J = 8.7 Hz), 7.35 (t, 1H, ar, J = 7.3 Hz), 7.54-7.57 (m, 4H, 2ar + $NH_2$), 7.65 (s, 1H, H-5), 7.98 (d, 2H, ar, J = 8.7 Hz), 8.07 (d, 2H, ar, J = 7.9 Hz). Anal. Calc. for $C_{21}H_{21}N_5O_2$.

*8-Amino-6-[(4-cyclopropylmethoxy)phenyl]-2-phenyl-1,2,4-triazolo[4,3-a]pyrazin-3(2H)-one* ***(24)***. Yield 86%; mp 276-278 °C (EtOH/2-Methoxyethanol). $^1$H NMR (DMSO-$d_6$) 0.32-0.36 (m, 2H, 2CH), 0.57-0.60 (m, 2H, 2CH), 1.21-1.24 (m, 1H, CH), 3.85 (d, 2H, $CH_2$, J = 7.0 Hz), 6.97 (d, 2H, ar, J = 8.9 Hz), 7.36 (t, 1H, ar, J = 7.4 Hz), 7.54 (br s, 2H, $NH_2$), 7.56 (t, 2H, ar, J = 7.4 Hz), 7.65 (s, 1H, H-5), 7.91 (d, 2H, ar, J = 8.9 Hz), 8.08 (d, 2H, ar, J = 7.4 Hz). IR 3362, 3316, 1669, 1649. Anal. Calc. for $C_{21}H_{19}N_5O_2$.

*8-Amino-6-[(4-cyclobutylmethoxy)phenyl]-2-phenyl-1,2,4-triazolo[4,3-a]pyrazin-3(2H)-one* ***(25)***. Yield 45%; mp 266-268 °C (EtOH/2-Methoxyethanol). $^1$H NMR (DMSO-$d_6$) 1.88-1.96 (m, 4H, 4CH), 2.06-2.13 (m, 2H, 2CH), 2.72-2.75 (m, 1H, CH), 3.99 (d, 2H, $CH_2$, J = 6.7 Hz), 6.98 (d, 2H, ar, J = 8.8 Hz), 7.36 (t, 1H, ar, J = 7.4 Hz), 7.56 (br s, 2H, $NH_2$), 7.60 (t, 2H, ar, J = 7.8 Hz), 7.65 (s, 1H, H-5), 7.90 (d, 2H, ar, J = 8.8 Hz), 8.08 (d, 2H, ar, J = 7.8 Hz). IR 3354, 3312, 1699, 1647. Anal. Calc. for $C_{22}H_{21}N_5O_2$.

*8-Amino-2-phenyl-6-(4-allyloxy)phenyl-1,2,4-triazolo[4,3-a]pyrazin-3(2H)-one* ***(26)***. Yield 75%; mp 260-261 °C (2-Methoxyethanol). $^1$H NMR (DMSO-$d_6$) 4.60 (d, 2H, $CH_2$), 5.27 (d, 1H, geminal CH=, J = 10.4 Hz), 5.42 (d, 1H, geminal CH=, J = 17.4 Hz), 6.02-6.11 (m, 1H, CH=), 7.00 (d, 2H,

ar, J = 8.8 Hz), 7.35 (t, 1H, ar, J = 7.9 Hz), 7.54-7.58 (m, 4H, 2ar + $NH_2$), 7.66 (s, 1H, H-5), 7.90 (d, 2H, ar, J = 8.8 Hz), 8.07 (d, 2H, ar, J = 7.9 Hz). Anal. Calc. for $C_{20}H_{17}N_5O_2$.

**General Procedure for the Synthesis of Ethyl 2-amino-2-arylhydrazonoacetates (31-34).**

Ethyl 2-amino-2-arylhydrazonoacetates **32** ($R_2$= 4-OMe), **33** ($R_2$= 2-OMe) and **34** ($R_2$= 4-$NO_2$)[36] were prepared as previously described for **31** (R= H)[35] i.e. from the corresponding 2-chloro derivatives **27-30**. Briefly, 33% aqueous ammonia (3 mL) in dioxane (5 mL) was added dropwise to a solution of derivatives **27-30**[23,33,34] (13.3 mmol) in dioxane (15 mL) and the reaction mixture was stirred for 4 h at rt. The white solid was filtered off and the mother liquor was concentrated at reduced pressure. The obtained precipitate was collected by filtration, washed with water (30 mL), dried and recrystallized. The crude compounds **32** and **33** were obtained as oily residues which were purified on silica gel column chromatography (eluent cyclohexane/EtOAc, 7:3 and 1:1, respectively). After evaporation of the eluent, derivative **32** was an oily product which was used as such for the next step while **33** solidified.

*Ethyl 2-amino-2-(phenylhydrazono)acetate (**31**)*. Yield 73%; mp 129-130 °C (lit[35] 128 °C) (Cyclohexane/EtOAc). $^1$H NMR (DMSO-$d_6$) 1.28 (t, 3H, ar, J = 7.1 Hz), 4.23 (q, 2H, $CH_2$, J = 7.1 Hz), 5.88 (br s, 2H, $NH_2$), 6.72 (t, 1H, ar, J = 7.3 Hz), 7.01 (d, 2H, ar, J = 7.6 Hz), 7.18 (t, 1H, ar, J = 8.2 Hz), 8.66 (br s, 1H, NH).

*Ethyl 2-amino-2-(4-methoxyphenylhydrazono)acetate (**32**)*. Yield 55%; brownish oil; $^1$H NMR ($CDCl_3$) 1.42 (t, 3H, $CH_3$, J = 7.1 Hz), 3.87 (s, 3H, $OCH_3$), 4.38 (q, 2H, $CH_2$, J = 7.1 Hz), 4.69 (br s, 2H, $NH_2$), 6.45 (br s, 1H, NH), 6.88 (d, 2H, ar, J= 9.0 Hz), 7.11 (d, 2H, ar, J= 9.0 Hz), 8.27 (s, 1H, NH).

*Ethyl 2-amino-2-(2-methoxyphenylhydrazono)acetate (**33**)*. Yield 95%; mp 99-101 °C (Cyclohexane/EtOAc). $^1$H- NMR (DMSO-$d_6$) 1.28 (t, 3H, ar, J = 7.1 Hz), 3.82 (s, 3H, $OCH_3$), 4.23 (q, 2H, $CH_2$, J = 7.1 Hz), 6.15 (br s, 2H, $NH_2$), 6.73 (t, 1H, ar, J = 7.6 Hz), 6.84-6.92 (m, 2H, ar), 7.28 (d, 1H, ar, J = 7.9 Hz), 7.86 (s, 1H, NH). Anal. Calcd. for $C_{11}H_{15}N_3O_3$.

*Ethyl 2-amino-2-(4-nitrophenylhydrazono)acetate (**34**)*. Yield 65 %; mp 192-193 °C (EtOH) (lit[36] 190-191 °C). $^1$H NMR (DMSO-$d_6$) 1.29 (t, 3H, $CH_3$, J = 7.2 Hz), 4.27 (q, 2H, $CH_2$, J = 7.2 Hz), 6.39 (br s, 2H, $NH_2$), 7.07 (d, 2H, ar, J = 9.2 Hz), 8.20 (d, 2H, ar, J = 9.2 Hz), 9.66 (br s, 1H, NH).

**General Procedure for the Synthesis of Ethyl 5-oxo-1-aryl-4,5-dihydro-1*H*-1,2,4-triazole-3-carboxylates (35-38).**

A solution of triphosgene (4.2 mmol) in anhydrous THF (10 mL) was added dropwise to a stirred solution of ethyl 2-amino-2-(arylhydrazono)acetate derivatives **31-34** (4.6 mmol) in anhydrous THF (15 mL) at 0 °C. After the addition was completed, the mixture was stirred 2-3 h at rt. Then, most of the solvent was removed at reduced pressure and water (20 mL) was added to the residue to give a solid which was collected by filtration, washed with water (20 mL), dried and recrystallized.

*Ethyl 5-oxo-1-phenyl-4,5-dihydro-1H-1,2,4-triazole-3-carboxylate (**35**)*. Yield 62%; mp 200-202 °C (lit.[37] 193-194 °C) (Cyclohexane/EtOAc). $^1$H NMR (DMSO-$d_6$) 1.33 (t, 3H, $CH_3$, J = 7.1 Hz), 4.38 (q, 2H, $CH_2$, J = 7.1 Hz), 7.30 (t, 1H, ar, J = 7.4 Hz), 7.49 (t, 2H, ar, J = 7.4 Hz), 7.89 (d, 2H, ar, J = 7.6 Hz), 7.90 (s, 1H, H-9), 12.99 (br s, 1H, NH).

*Ethyl 1-(4-methoxyphenyl)-5-oxo-4,5-dihydro-1H-1,2,4-triazole-3-carboxylate (**36**)*. Yield 42%; mp 186-187 °C (lit[37] 179 °C) (EtOH). $^1$H NMR ($CDCl_3$) 1.48 (t, 3H, $CH_3$, J = 7.2 Hz), 3.80 (s, 3H, $OCH_3$),4.50 (q, 2H, $CH_2$, J = 7.2 Hz), 6.98 (d, 2H, ar, J = 9.1 Hz), 7.87 (d, 2H, ar, J = 9.1 Hz), 10.65 (br s, 1H, NH).

*Ethyl 1-(2-methoxyphenyl)-5-oxo-4,5-dihydro-1H-1,2,4-triazole-3-carboxylate (**37**)*. Yield 79%; mp 131-133 °C (EtOAc). $^1$H NMR (DMSO-$d_6$) 1.30 (t, 3H, $CH_3$, J = 7.1 Hz), 3.78 (s, 3H, $OCH_3$), 4.34 (q, 2H, $CH_2$, J = 7.1 Hz), 7.06 (t, 1H, ar, J = 7.6 Hz), 7.21 (d, 1H, ar, J= 8.3 Hz), 7.36 (d, 1H, J = 7.6 Hz), 7.49 (t, 1H, J = 7.6 Hz), 12.69 (br s, 1H, NH). Anal. Calcd. for $C_{12}H_{13}N_3O_4$.

*Ethyl 1-(4-nitrophenyl)-5-oxo-4,5-dihydro-1H-1,2,4-triazole-3-carboxylate (**38**)*. Yield 65%; mp 241-242 °C (Cyclohexane/EtOAc). $^1$H NMR ($CDCl_3$) 1.50 (t, 3H, $CH_3$, J = 7.1 Hz,), 4.55 (q, 2H,

$CH_2$, J = 7.1 Hz), 8.29-8.37 (m, 4H, ar), 10.31 (br s, 1H, NH). IR 3369, 1755, 1698, 1513, 1375. Anal. Calcd. for $C_{11}H_{10}N_4O_5$.

**General Procedure for the Synthesis of Ethyl 1-aryl-5-oxo-4-(2-oxopropyl)-4,5-dihydro-1*H*-1,2,4-triazole-3-carboxylates (39, 41) and Ethyl 1-aryl-5-oxo-4-(2-oxoarylethyl)-4,5-dihydro-1*H*-1,2,4-triazole-3-carboxylates (40, 42-47).**

Chloroacetone (1.2 mmol) or the suitable α-bromoketone (1.2 mmol) was added to a mixture of ethyl 1-aryl-5-oxo-1,2,4-triazole-3-carboxylate derivatives **35-38** (1 mmol) and potassium carbonate (2 mmol) in DMF/$CH_3CN$ (1:9 ratio, 10 mL). The suspension was stirred at rt until the disappearance of the starting material (TLC monitoring, 2-24 h). The solvent was removed at reduced pressure and the residue was treated with water (50-70 mL). The solid was collected by filtration, washed with water (20 mL), then with $Et_2O$ (10 mL) and recrystallized. To isolate compound **44**, the reaction mixture was treated with water (50-70 mL) and extracted with $CH_2Cl_2$ (30 mL x 3). The organic phase was anhydrified ($Na_2SO_4$) and reduced to dryness under vacuum to give a solid made up of a mixture of derivative **44** and its O-alkylated isomer **44a** (about 2:0.8 ratio, from $^1$H NMR spectrum) that were separated on silica gel column (eluent n-hexane/EtOAc/$Et_2O$ 5:4:7). Compounds **44** and **44a** were obtained, respectively from the second and first eluates.

*Ethyl 5-oxo-4-(2-oxopropyl)-1-phenyl-4,5-dihydro-1H-1,2,4-triazole-3-carboxylate (**39**)*. Yield 58%; mp 104-105 °C (EtOH). $^1$H NMR (DMSO-$d_6$) 1.31 (t, 3H, $CH_3$, J = 7.1 Hz), 2.28 (s, 3H, $CH_3$), 4.35 (q, 2H, $CH_2$, J = 7.1 Hz), 4.92 (s, 2H, $CH_2$), 7.35 (t, 1H, ar, J = 7.4 Hz), 7.54 (t, 2H, ar, J = 7.4 Hz), 7.91 (d, 2H, ar, J = 7.7 Hz). Anal. Calc. for $C_{14}H_{15}N_3O_4$.

*Ethyl 5-oxo-4-(2-oxo-2-phenylethyl)-1-phenyl-4,5-dihydro-1H-1,2,4-triazole-3-carboxylate (**40**)*. Yield 75%; mp 157-159 °C (EtOAc/EtOH). $^1$H NMR (DMSO-$d_6$) 1.21 (t, 3H, ar, J = 7.1 Hz), 4.29 (q, 2H, $CH_2$, J = 7.1 Hz), 5.59 (s, 2H, $CH_2$), 7.37 (t, 1H, ar, J = 7.4 Hz), 7.55 (t, 2H, ar, J = 7.6 Hz), 7.63 (t, 2H, ar, J = 7.7 Hz), 7.76 (t, 1H, ar, J = 7.4 Hz), 7.95 (d, 2H, ar, J = 7.7 Hz), 8.11 (d, 2H, ar, J = 7.8 Hz). Anal. Calc. for $C_{19}H_{17}N_3O_4$.

*Ethyl 1-(4-methoxyphenyl)-5-oxo-4-(2-oxopropyl)-4,5-dihydro-1H-1,2,4-triazole-3-carboxylate (**41**)*. Yield 92%; mp 98-100 °C (EtOH). $^1$H NMR (DMSO-$d_6$) 1.30 (t, 3H, $CH_3$, J = 7.1 Hz), 2.27 (s, 3H, $CH_3$), 3.80 (s, 3H, $OCH_3$), 4.34 (q, 2H, $CH_2$, J = 7.1 Hz), 4.91 (s, 2H, $CH_2$), 7.08 (d, 2H, ar, J = 9.1 Hz), 7.76 (d, 2H, ar, J = 9.1 Hz). Anal. Calc. for $C_{15}H_{17}N_3O_5$.

*Ethyl 1-(4-methoxyphenyl)-5-oxo-4-(2-oxo-2-phenylethyl)-4,5-dihydro-1H-1,2,4-triazole-3-carboxylate (**42**)*. Yield 58%; mp 127-128 °C (Cyclohexane/EtOAc). $^1$H NMR ($CDCl_3$) 1.38 (t, 3H, $CH_3$, J = 7.1 Hz), 3.86 (s, 3H, $OCH_3$), 4.40 (q, 2H, $CH_2$, J = 7.1 Hz), 5.57 (s, 2H, $CH_2$), 6.99 (d, 2H, ar, J = 9.1 Hz), 7.55 (t, 2H, ar, J = 7.5 Hz), 7.68 (t, 1H, ar, J = 7.4 Hz), 7.88 (d, 2H, ar, J = 9.1 Hz), 8.03 (d, 2H, ar, J = 7.4 Hz). IR 1732, 1711, 1694. Anal. Calc. for $C_{20}H_{19}N_3O_5$.

*Ethyl 1-(4-nitrophenyl)-5-oxo-4-(2-oxo-2-phenylethyl)-4,5-dihydro-1H-1,2,4-triazole-3-carboxylate (**43**)*. Yield 92 %; mp 147-148 °C (MeOH). $^1$H NMR ($CDCl_3$) 1.40 (t, 3H, $CH_3$, J = 7.2 Hz), 4.44 (q, 2H, $CH_2$, J = 7.2 Hz), 5.59 (s, 2H, $CH_2$), 7.58 (t, 2H, ar, J = 7.2 Hz), 7.70 (t, 1H, ar, J = 8.4 Hz), 8.04 (d, 2H, ar, J = 7.2 Hz), 8.35-8.38 (m, 4H, ar). IR 1736, 1725, 1700, 1463, 1375. Anal. Calc. for $C_{19}H_{16}N_4O_6$.

*Ethyl 1-(2-methoxyphenyl)-5-oxo-4-(2-oxo-2-phenylethyl)-4,5-dihydro-1H-1,2,4-triazole-3-carboxylate (**44**)*. Yield 65 %; mp 88-90 °C (Cyclohexane/EtOAc). $^1$H NMR (DMSO-$d_6$) 1.18 (t, 3H, $CH_3$, J = 7.1 Hz), 3.81 (s, 3H, $OCH_3$), 4.24 (q, 2H, $CH_2$, J = 7.1 Hz), 5.55 (s, 2H, $CH_2$), 7.04-7.09 (m, 2H, ar), 7.42-7.48 (m, 2H, ar), 7.57 (t, 2H, ar, J = 7.5 Hz), 7.67 (t, 1H, ar, J = 7.4 Hz), 8.04 (d, 2H, ar, J = 7.1 Hz). Anal. Calc. for $C_{20}H_{19}N_3O_5$.

*Ethyl 1-(2-methoxyphenyl)-5-(2-oxo-2-phenylethoxy)-1H-1,2,4-triazole-3-carboxylate (**44a**)*. Yield 30 %; mp 138-140 °C (Cyclohexane/EtOAc). $^1$H NMR (DMSO-$d_6$) 1.27 (t, 3H, $CH_3$, J= 7.1 Hz), 3.84 (s, 3H, $OCH_3$), 4.29 (q, 2H, $CH_2$, J = 7.1 Hz), 5.94 (s, 2H, $CH_2$), 7.15 (t, 1H, ar, J = 7.6 Hz), 7.30 (d, 1H, ar, J = 7.8 Hz), 7.52 (d, 1H, ar, J = 7.8 Hz), 7.58 (t, 2H, ar, J = 7.8 Hz), 7.73 (t, 1H, ar, J = 7.4 Hz), 7.98 (d, 2H, ar, J = 7.8 Hz). Anal. Calc. for $C_{20}H_{19}N_3O_5$.

*Ethyl 4-[2-(3-methoxyphenyl)-2-oxoethyl]-5-oxo-1-phenyl-4,5-dihydro-1H-1,2,4-triazole-3-carboxylate (**45**)*. Yield 80%; mp 123-125 °C (EtOH). $^1$H NMR (DMSO-$d_6$) 1.20 (t, 3H, ar, J = 7.1

Hz), 3.86 (s, 3H, $OCH_3$), 4.29 (q, 2H, $CH_2$, J = 7.1 Hz), 5.59 (s, 2H, $CH_2$), 7.34-7.38 (m, 2H, ar), 7.52-7.57 (m, 4H, ar), 7.71 (d, 1H, ar, J = 7.7 Hz), 7.94 (d, 2H, ar, J = 8.0 Hz). Anal. Calc. for $C_{20}H_{19}N_3O_5$.

*Ethyl 4-[2-(4-methoxyphenyl)-2-oxoethyl]-5-oxo-1-phenyl-4,5-dihydro-1H-1,2,4-triazole-3-carboxylate (**46**)*. Yield 85%; mp 149-151 °C (Cyclohexane/EtOAc). $^1$H NMR ($CDCl_3$) 1.38 (t, 3H, $CH_3$, J = 6.9 Hz), 3.93 (s, 3H, $CH_3$), 4.41 (q, 2H, $CH_2$, J = 6.9 Hz), 5.53 (s, 2H, $CH_2$), 7.02 (d, 2H, $CH_2$, J = 7.6 Hz), 7.31 (t, 1H, ar, J = 7.4 Hz), 7.48 (t, 2H, ar, J = 7.4 Hz), 8.01-8.05 (m, 4H, ar). Anal. Calc. for $C_{20}H_{19}N_3O_5$.

*Ethyl 4-[2-(4-methylphenyl)-2-oxoethyl]-5-oxo-1-phenyl-4,5-dihydro-1H-1,2,4-triazole-3-carboxylate (**47**)*. Yield 60%; mp 189-190 °C (EtOH). $^1$H NMR (DMSO-$d_6$) 1.19 (t, 3H, $CH_3$, J = 6.9 Hz), 2.43 (s, 3H, $CH_3$) 4.28 (q, 2H, $CH_2$, J = 7.1 Hz), 5.55 (s, 2H, $CH_2$), 7.37 (t, 1H, ar, J = 7.4 Hz), 7.43 (d, 2H, ar, J = 7.7 Hz), 7.55 (t, 2H, ar, J = 7.7 Hz), 7.94 (d, 2H, ar, J = 8.3 Hz), 8.01 (d, 2H, ar, J = 7.6 Hz). Anal. Calc. for $C_{20}H_{19}N_3O_4$.

**General Procedure for the Synthesis of 1,2,4-Triazolo[4,3-*a*]pyrazine-3,8(2*H*,7*H*)-dione derivatives (48-53).**

A mixture of the suitable ethyl 1,2,4-triazole-3-carboxylate derivatives **39-44** (0.87 mmol) and ammonium acetate (3.48 mmol) was heated under the following conditions: microwave irradiation at 140 °C for 10 min (**48**, **49**) or for 1 h and 45 min (**50**) otherwise in a sealed tube at 130 ° for 6 h (**53**) or at 190 °C for about 20 h (**51**, **52**). The obtained mixture was cooled at room temperature and taken up with EtOH (1 mL) and $Et_2O$ (5 mL). The resulting solid was collected by filtration and washed with water (20 mL). All the crude compounds were purified by recrystallization.

*6-Methyl-2-phenyl-1,2,4-triazolo[4,3-a]pyrazine-3,8(2H,7H)-dione (**48**).* Yield 85%; mp 288-289 °C (2-Methoxyethanol). $^1$H NMR (DMSO-$d_6$) 2.04 (s, 3H, $CH_3$), 6.88 (s, 1H, H-5), 7.34 (t, 1H, ar, J

= 7.4 Hz), 7.54 (t, 2H, ar, J = 7.8 Hz), 7.98 (d, 2H, ar, J = 8.3 Hz), 11.32 (br s, 1H, NH). Anal. Calc. for $C_{12}H_{10}N_4O_2$.

*2,6-Diphenyl-1,2,4-triazolo[4,3-a]pyrazine-3,8(2H,7H)-dione (**49**)*. Yield 65%; mp 290-291 °C (2-Methoxyethanol). $^1$H NMR (DMSO-$d_6$) 7.28 (s, 1H, H-5), 7.37 (t, 1H, ar, J = 7.4 Hz), 7.46-7.51 (m, 3H, ar,), 7.57 (t, 2H, ar, J = 7.7 Hz), 7.72 (d, 2H, ar, J = 8.0 Hz), 8.02 (d, 2H, ar, J = 7.9 Hz), 11.63 (br s, 1H, NH). Anal. Calc. for $C_{17}H_{12}N_4O_2$.

*6-Methyl-2-(4-methoxyphenyl)-1,2,4-triazolo[4,3-a]pyrazine-3,8(2H,7H)-dione (**50**)*. Yield 78%; mp > 300 °C (DMF). $^1$H NMR (DMSO-$d_6$) 2.04 (s, 3H, $CH_3$), 3.80 (s, 3H, $OCH_3$), 6.87 (s, 1H, H-5), 7.09 (d, 2H, ar, J = 9.1 Hz), 7.85 (d, 2H, ar, J = 9.1 Hz), 11.30 (br s, 1H, NH). Anal. Calc. for $C_{13}H_{12}N_4O_3$.

*2-(4-Methoxyphenyl)-6-phenyl-1,2,4-triazolo[4,3-a]pyrazine-3,8(2H,7H)-dione (**51**)*. Yield 75%; mp >300 °C (DMF). $^1$H NMR (DMSO-$d_6$) 3.82 (s, 3H, $OCH_3$), 7.14 (d, 2H, ar, J = 9.0 Hz), 7.26 (s, 1H, H-5) 7.46-7.51 (m, 3H, ar), 7.71 (d, 2H, ar, J = 6.2 Hz), 7.88 (d, 2H, ar, J = 9.0 Hz), 11.60 (br s, 1H, NH). IR 3218, 1688. Anal. Calc. for $C_{18}H_{14}N_4O_3$.

*2-(4-Nitrophenyl)-6-phenyl-1,2,4-triazolo[4,3-a]pyrazine-3,8(2H,7H)-dione (**52**)*. Yield 92 %; mp > 300 °C (DMF). $^1$H NMR (DMSO-$d_6$) 7.32 (s, 1H, H-5), 7.47-7.50 (m, 3H, ar), 7.72-7.74 (m, 2H, ar), 8.34 (d, 2H, ar, J = 9.2 Hz), 8.46 (d, 2H, ar, J = 9.2 Hz), 11.71 (br s, 1H, NH). IR 3260, 1686. Anal. Calc. for $C_{17}H_{11}N_5O_4$.

*2-(2-Methoxyphenyl)-6-phenyl-1,2,4-triazolo[4,3-a]pyrazine-3,8(2H,7H)-dione (**53**)*. Yield 85%; mp > 300 °C (2-Methoxyethanol). $^1$H NMR (DMSO-$d_6$) 3.99 (s, 3H, $OCH_3$), 7.12 (t, 1H, ar, J = 7.1 Hz), 7.23 (s, 1H, H-5), 7.27 (d, 1H, ar, J = 7.7 Hz), 7.44-7.50 (m, 4H, ar), 7.53 (t, 1H, ar, J = 8.5 Hz), 7.71 (s, 2H, ar, J = 8.2 Hz), 11.60 (br s, 1H, NH). IR 3259, 1714, 1689. Anal. Calc. for $C_{18}H_{14}N_4O_3$.

**General Procedure for the Synthesis of 2-(Hydroxyphenyl)-substituted 1,2,4-triazolo[4,3-*a*]pyrazine-3,8(2*H*,7*H*)-dione derivatives (54-56).**

A solution of $BBr_3$ in dichloromethane (1M, 5.1 mL) was slowly added at 0 °C, under nitrogen atmosphere, to a suspension of the methoxyphenyl-substituted triazolopyrazine derivatives **50, 51** and **53** (1.02 mmol) in anhydrous dichloromethane (20 mL). The mixture was stirred at rt until the disappearance of the starting material (TLC monitoring, 5-16 h), then was diluted with water (10 mL) and neutralized with a $NaHCO_3$ saturated solution. The organic solvent was removed by evaporation at reduced pressure and the solid was collected by filtration. The crude derivative was dried and purified by recrystallization.

*2-(4-Hydroxyphenyl)-6-methyl-1,2,4-triazolo[4,3-a]pyrazine-3,8(2H,7H)-dione (**54**).* Yield 74%; mp > 300 °C (DMF/AcOH). $^1$H NMR (DMSO-$d_6$) 2.03 (s, 3H, $CH_3$), 6.87 (s, 1H, H-5), 6.89 (d, 2H, ar, J = 6.9 Hz), 7.70 (d, 2H, ar, J = 6.70 Hz), 9.72 (br s, 1H, OH), 11.54 (br s, 1H, NH). Anal. Calc. For $C_{12}H_{10}N_4O_3$.

*2-(4-Hydroxyphenyl)-6-phenyl-1,2,4-triazolo[4,3-a]pyrazine-3,8(2H,7H)-dione (**55**).* Yield 75%; mp > 300 °C (EtOH). $^1$H NMR (DMSO-$d_6$) 6.91 (d, 2H, ar, J = 7.7 Hz), 7.25 (s, 1H, H-5), 7.45-7.49 (m, 3H, ar), 7.7-7.75 (m, 4H, ar), 9.74 (br s, 1H, OH), 11.60 (br s, 1H, NH). Anal. Calc. For $C_{17}H_{12}N_4O_3$.

*2-(2-Hydroxyphenyl)-6-phenyl-1,2,4-triazolo[4,3-a]pyrazine-3,8(2H,7H)-dione (**56**).* Yield 83%; mp 270-271 °C ( 2-Methoxyethanol). $^1$H NMR (DMSO-$d_6$) 6.95 (t, 1H, ar, J = 7.5 Hz), 7.03 (d, 1H, ar, J = 7.5 Hz), 7.27 (s, 1H, H-5), 7.53 (d, 2H, ar, J = 7.5 Hz), 7.44-7.50 (m, 3H, ar), 7.72 (d, 2H, ar, J = 7.5 Hz), 9.93 (s, 1H, OH), 11.59 (br s, 1H, NH). IR 3178, 3122, 1701, 1670. Anal. Calc. For $C_{17}H_{12}N_4O_3$.

**2-(4-Aminophenyl)-6-phenyl-1,2,4-triazolo[4,3-*a*]pyrazine-3,8(2*H*,7*H*)-dione (57)**.

10 % Pd/C (10% w/w with respect to the nitro derivative) was added to a solution of the 2-(4-nitrophenyl) derivative **52** (1.2 mmol) in DMF (6 mL). The mixture was hydrogenated in a Parr apparatus at 40 psi for 20 h. Then the catalyst was filtered off and the clear solution was diluted with water (about 50 mL) to obtain a solid that was collected by filtration, washed with water and

$Et_2O$, dried and recrystallized. Yield 46%; mp 285-286 °C (EtOH/EtOAc). $^1$H NMR (DMSO-$d_6$) 5.34 (br s, 2H, $NH_2$), 6.67 (d, 2H, ar, J = 8.6 Hz), 7.23 (s, 1H, H-5), 7.44-7.48 (m, 3H, ar), 7.54 (d, 2H, ar, J = 8.6 Hz),7.70 (d, 2H, ar, J = 7.7 Hz), 11.56 (br s, 1H, NH). IR 3476, 3375, 3246, 1685. Anal. Calc. For $C_{17}H_{13}N_5O_2$.

**General Procedure for the Synthesis of 1,2,4-Triazolo[4,3-*a*]pyrazine-3,8(2*H*,7*H*)-dione derivatives (58-60).**

The title compounds were prepared by reacting the suitable ethyl 1,2,4-triazole-3-carboxylate derivatives **45-47** (0.87 mmol) and ammonium acetate (3.48 mmol) under microwave irradiation at 140 °C for 1 h and 45 min, following the procedure described above to prepare derivatives **48-53**. The crude products were purified by recrystallization.

*6-(3-Methoxyphenyl)-2-phenyl-1,2,4-triazolo[4,3-a]pyrazine-3,8(2H,7H)-dione (**58**)*. Yield 79%; mp> 300 °C (2-Methoxyethanol). $^1$H NMR (DMSO-$d_6$) 3.85 (s, 3H, $OCH_3$), 6.99-7.02 (m, 1H, ar), 7.27-7.30 (m, 2H, ar), 7.35-7.40 (m, 3H, 1 ar + H-5), 7.57 (t, 2H, ar, J = 7.1 Hz), 8.02 (d, 2H, ar, J = 8.6 Hz), 11.60 (s, 1H, NH). Anal. Calc. for $C_{18}H_{14}N_4O_3$.

*6-(4-Methoxyphenyl)-2-phenyl-1,2,4-triazolo[4,3-a]pyrazine-3,8(2H,7H)-dione (**59**)*. Yield 70%; mp 290-291 °C (2-Methoxyethanol). $^1$H NMR (DMSO-$d_6$) 3.82 (s, 3H, $OCH_3$), 7.03 (d, 2H, ar, J = 8.8 Hz), 7.19 (s, 1H, H-5), 7.36 (t, 1H, ar, J = 7.4 Hz), 7.56 (t, 2H, ar, J = 8.0 Hz), 7.66 (d, 2H, ar, J = 8.8 Hz), 8.02 (d, 2H, ar, J = 7.8 Hz), 11.55 (br s, 1H, NH). IR 3229, 1682 $cm^{-1}$. Anal. Calc. for $C_{18}H_{14}N_4O_3$.

*6-(4-Methylphenyl)-2-phenyl-1,2,4-triazolo[4,3-a]pyrazine-3,8(2H,7H)-dione (**60**)*. Yield 80%; mp > 300 °C (EtOH/2-Methoxyethanol). $^1$H NMR (DMSO-$d_6$) 2.36 (s, 3H, $CH_3$), 7.23 (s, 1H, H-5), 7.29 (d, 2H, ar, J = 8.0 Hz), 7.37 (t, 1H, ar, J = 7.1 Hz), 7.54-7.62 (m, 4H, ar), 8.02 (d, 2H, ar, J = 8.5 Hz), 11.59 (br s, 1H, NH). IR 3387, 1688. Anal. Calc. For $C_{18}H_{14}N_4O_2$.

**6-(3-Hydroxyphenyl)-2-phenyl-1,2,4-triazolo[4,3-*a*]pyrazine-3,8(2H,7H)-dione (61)**.

The title compound was obtained by reacting the corresponding methoxy derivative **58** (1.02 mmol) with $BBr_3$ in the same experimental conditions as described above to prepare **54-56**. Yield 94%; mp >300 °C (2-Methoxyethanol/EtOH). $^1$H NMR (DMSO-$d_6$) 6.86 (d, 1H, ar, J = 7.9 Hz), 7.02 (s, 1H, ar), 7.04-7.12 (m, 2H, 1 ar + H-5), 7.28 (t, 1H, ar, J = 7.9 Hz), 7.37 (t, 1H, ar, J = 7.6 Hz), 7.56 (t, 2H, ar, J = 7.6 Hz), 8.02 (d, 2H, ar, J = 7.6 Hz), 9.69 (s, 1H, OH), 11.55 (br s, 1H, NH). IR 3366, 1682, 1661. Anal. Calc. For $C_{17}H_{12}N_4O_3$.

**6-(4-Hydroxyphenyl)-2-phenyl-1,2,4-triazolo[4,3-*a*]pyrazine-3,8(2*H*,7*H*)-dione (62)**. A suspension of the 6-(4-methoxyphenyl) derivative **59** (0.45 mmol) in glacial acetic acid (6 mL) and 48% HBr solution (4.2 mL) was heated at reflux for 24 h. After cooling at room temperature, the mixture was diluted with water (about 15 mL) to give a solid which was collected by filtration, washed with water and recristallized. Yield 80%; mp > 300 °C (2-Methoxyethanol/EtOH). $^1$H NMR (DMSO-$d_6$) 6.84 (d, 2H, ar, J = 8.6 Hz), 7.10 (s, 1H, $H_5$), 7.36 (t, 1H, ar, J = 7.4 Hz), 7.52 (d, 2H, ar, J = 8.6 Hz), 7.56 (t, 1H, ar, J = 7.7 Hz), 8.02 (d, 2H, ar, J = 7.7 Hz), 9.84 (s, 1H, OH), 11.50 (br. s, 1H, NH). Anal. Calc. For $C_{17}H_{12}N_4O_3$.

**General Procedure for the Synthesis of 8-Chloro-2-phenyl-1,2,4-triazolo[4,3-*a*]pyrazin-3-(2*H*)-one derivatives (63-71).**

A suspension of the suitable triazolopyrazine-3,8-dione derivatives **48-53, 58-60** (2 mmol) in phosphorus oxychloride (10 mL) was heated in the following conditions: microwave irradiation at 160 °C for 20 min (compound **64**), 1 h (compound **67**) and 3.5 h (compound **68**) or at 170 °C for 30 min (compound **69**) and 1.5 h (compounds **70** and **71**); sealed tube in a bath oil at 140 °C for 16 h (compounds **63** and **65**) or at 180 °C for 3 h (compound **66**). The excess of phosphorus oxychloride was distilled off and the residue was treated with water (about 5−10 mL). The obtained solid was

collected by filtration. These intermediates were pure enough (NMR, TLC) to be used for the next step without further purification.

*8-Chloro-6-methyl-2-phenyl-1,2,4-triazolo[4,3-a]pyrazin-3(2H)-one (**63**).* Yield 81%; $^1$H NMR (DMSO-$d_6$) 2.21 (s, 3H, $CH_3$), 7.47 (s, 1H, H-5), 7.55-7.58 (m, 1H, ar), 7.54 (t, 2H, ar, J = 7.7 Hz), 8.01-8.3 (m, 2H, ar).

*8-Chloro-2,6-diphenyl-1,2,4-triazolo[4,3-a]pyrazin-3(2H)-one (**64**).* Yield 78%; $^1$H NMR (DMSO-$d_6$) 7.41-7.43 (m, 2H, ar), 7.50 (t, 2H, ar, J = 7.3 Hz), 7.60 (t, 2H, ar, J = 8.0 Hz), 8.04-8.09 (m, 4H, ar), 8.61 (s, 1H, H-5).

*8-Chloro-6-methyl-2-(4-methoxyphenyl)-1,2,4-triazolo[4,3-a]pyrazin-3(2H)-one (**65**).* Yield 80%; $^1$H NMR (DMSO-$d_6$) 2.31 (s, 3H, $CH_3$), 3.82 (s, 3H, $OCH_3$), 7.12 (d, 2H, ar, J = 8.0 Hz), 7.90-7.93 (m, 3H, 2 ar + H-5).

*8-Chloro-2-(4-methoxyphenyl)-6-phenyl-1,2,4-triazolo[4,3-a]pyrazin-3(2H)one (**66**).* Yield 96%; $^1$H NMR (DMSO-$d_6$) 3.84 (s, 3H, $OCH_3$), 7.15 (d, 2H, ar, J = 9.1 Hz), 7.04-7.63 (m, 3H, ar), 7.94 (d, 2H, ar, J= 9.1 Hz), 8.05 (d, 2H, ar, J = 7.5 Hz), 8.61 (s, 1H, H-5).

*8-Chloro-2-(4-nitrophenyl)-6-phenyl-1,2,4-triazolo[4,3-a]pyrazin-3(2H)one (**67**).* Yield 72%; $^1$H NMR (DMSO-$d_6$) 7.42 (t, 1H, ar, J = 7.4 Hz), 7.51 (d, 2H, ar, J = 7.4 Hz), 8.07 (d, 2H, ar, J = 7.4 Hz), 8.39 (d, 2H, ar, J = 7.1 Hz), 8.47 (d, 2H, ar, J = 7.1 Hz), 8.67 (s, 1H, H-5).

*8-Chloro-2-(2-methoxyphenyl)-6-phenyl-1,2,4-triazolo[4,3-a]pyrazin-3(2H)one (**68**).* Yield 96%; $^1$H NMR (DMSO-$d_6$) 3.83 (s, 3H, $OCH_3$), 7.14 (t, 1H, ar, J = 7.6 Hz), 7.30 (d, 1H, ar, J = 8.4 Hz), 7.42 (t, 1H, ar, J = 7.3 Hz), 7.46-7.55 (m, 1H; ar), 7.57 (t, 1H, ar), 8.02 (d, 2H, ar, J = 7.3 Hz), 8.56 (s, 1H, H-5).

*8-Chloro-6-(3-methoxyphenyl)-2-phenyl-1,2,4-triazolo[4,3-a]pyrazin-3(2H)-one (**69**).* Yield 87%; $^1$H NMR (DMSO-$d_6$) 3.85 (s, 3H, $OCH_3$), 6.98 (d, 1H, ar, J = 7.6 Hz), 7.38-7.42 (m, 2H, ar), 7.57-7.63 (m, 4H, ar), 8.07 (d, 2H, ar, J = 7.7 Hz), 8.68 (s, 1H, H-5).

*8-Chloro-6-(4-methoxyphenyl)-2-phenyl-1,2,4-triazolo[4,3-a]pyrazin-3(2H)-one (**70**).* Yield 92%; $^1$H NMR (DMSO-$d_6$) 3.82 (s, 3H, $OCH_3$), 7.05 (d, 2H, ar, J = 8.8 Hz), 7.40 (t, 1H, ar, J = 7.4 Hz),

7.59 (t, 2H, ar, J = 7.9 Hz), 7.98 (d, 2H, ar, J = 8.8 Hz), 8.07 (d, 2H, ar, J = 7.9 Hz), 8.49 (s, 1H, H-5).

*8-Chloro-6-(4-methylphenyl)-2-phenyl-1,2,4-triazolo[4,3-a]pyrazin-3(2H)-one (**71**).* Yield 90%; $^1$H NMR (DMSO-$d_6$) 2.36 (s, 3H, $CH_3$), 7.30 (d, 2H, ar, J = 8.1 Hz), 7.40 (t, 1H, ar, J = 7.8 Hz), 7.59 (t, 2H, ar, J = 7.8 Hz), 7.94 (d, 2H, ar, J = 8.1 Hz), 8. 07 (d, 2H, ar, J = 8.5 Hz), 8.55 (s, 1H, H-5).

**Molecular Modeling**

*Refinement of the $hA_{2A}$ AR and $hA_1$ AR structures.* Two crystal structures of the $hA_{2A}$ AR in complex with the $hA_{2A}$ AR antagonist **72** were retrieved from the Protein Data Bank (http://www.rcsb.org; pdb code: 3EML; 2.6-Å resolution and pdb code: 4EIY; 1.8-Å resolution[55-57]). The 3EML crystal structure was re-modelled by firstly removing the T4L external segment and secondly by performing a building of missing receptor regions (i.e. missing sections of EL2 or IL3 domains). The Homology Modelling tool of MOE was employed. In detail, the boundaries identified from the used $hA_{2A}$ AR X-ray crystal structure were applied and the missing loop domains were built by the loop search method implemented in MOE.[51] Once the heavy atoms were modelled, all hydrogen atoms were added, and the protein coordinates were then minimized with MOE using the AMBER12:EHT force field. The minimizations were performed by steepest descent steps followed by conjugate gradient minimization until the root mean square (RMS) gradient of the potential energy was less than 0.05 kJ $mol^{-1}$ $Å^{-1}$. Reliability and quality of the model were checked using the Protein Geometry Monitor application within MOE, which provides a variety of stereochemical measurements for inspection of the structural quality in a given protein, like backbone bond lengths, angles and dihedrals, Ramachandran φ-ψ dihedral plots, and sidechain-rotamer and non-bonded contact quality. The 4EIY crystal structure was used in its original form to which all hydrogen atoms were added within MOE. The crystal structure of the $hA_1$ AR covalently bound to an antagonist was retrieved from the Protein Data Bank (pdb code: 5UEN; 3.2-Å resolution).[58] The

structure was prepared for docking studies following analogue protocol as described for the two $hA_{2A}$ AR structures.

*Homology modeling of the $hA_3$ AR structure*. A homology model of the $hA_3$ AR was built using the above cited X-ray structure of the antagonist-bound $A_1$ AR as template (pdb code: 5UEN). A multiple alignment of the AR primary sequences was built within MOE as preliminary step. The Homology Modelling tool of MOE was employed even for this task. The protocol followed by the tool is described above.

*Molecular docking analysis.* All compound structures were docked into the binding site of the hAR structures using three docking tools: the Induced Fit docking protocol of MOE, the genetic algorithm docking tool of CCDC Gold,[52] and the Lamarckian genetic algorithm of Autodock.[53,54] The Induced Fit docking protocol of MOE is divided into a number of stages: *Conformational Analysis of ligands*. The algorithm generated conformations from a single 3D conformation by conducting a systematic search. In this way, all combinations of angles were created for each ligand. *Placement*. A collection of poses was generated from the pool of ligand conformations using Alpha Triangle placement method. Poses were generated by superposition of ligand atom triplets and triplet points in the receptor binding site. The receptor site points are alpha sphere centers which represent locations of tight packing. At each iteration, a random conformation was selected, a random triplet of ligand atoms and a random triplet of alpha sphere centers were used to determine the pose. *Scoring*. Poses generated by the placement methodology were scored using the *Alpha HB* scoring function, which combines a term measuring the geometric fit of the ligand to the binding site and a term measuring hydrogen bonding effects. *Induced Fit*. The generated docking conformations were subjected to energy minimization within the binding site and the protein sidechains are included in the refinement stage. In detail, the protein backbone is set as rigid while the side chains are not set to “free to move” but are set to “tethered”, where an atom tether is a distance restraint that restrains the distance not between two atoms but between an atom and a fixed point in space. *Rescoring*. Complexes generated by the Induced Fit methodology stage were scored

using the *Alpha HB* scoring function. Gold tool was used with default efficiency settings through MOE interface, by selecting GoldScore as scoring function.[52] Autodock 4.2.6 software was used with PyRx interface. Lamarckian genetic algorithm was employed for this analysis with the following settings: 50 runs for each ligand; 2,500,000 as maximum number of energy evaluations; 27,000 as maximum number of generations; 0.02 as rate of gene mutation and 0.8 as rate of crossover. The grid box was set with 50, 50, and 50 points in the *x*, *y*, and *z* directions, respectively, with the default grid spacing of 0.375 Å.[53,54,63]

*Post Docking analysis. Residue interaction analysis.* The interactions between the ligands and the $hA_{2A}$ AR receptors binding site were analyzed by using the *IF-E 6.0* tool retrievable at the SVL exchange service (Chemical Computing Group, Inc. SVL exchange: http://svl.chemcomp.com). The program calculates and displays the atomic and residue interaction forces as 3D vectors. It also calculates the per-residue interaction energies, where negative and positive energy values are associated to favorable and unfavorable interactions, respectively. For each $hA_{2A}$ AR structure, a shell of residues contained within a 10 Å distance from ligand were considered for this analysis.

**Binding assays**

*Cell culture.* CHO cells stable transfected with hARs were grown in Dulbecco's modified Eagle's medium (DMME) with nutrient mixture F12 supplemented with 10% fetal bovine serum (FBS), 100 U/ml penicillin, 100 µg/ml streptomycin, 2.5 µg/ml Amphotericin B, 0.1 mg/ml Geneticine and 1 mM Sodium Pyruvate. They were cultured at 37 °C in a humidified atmosphere of 5% $CO_2$/95% air.[64]

*Membrane preparation.* Crude membranes for radioligand binding experiments were prepared by collecting cells (CHO stably transfected with $hA_1$, $hA_{2A}$ and $hA_3$ ARs) in ice-cold hypotonic buffer (5 mM Tris/HCl, 2 mM EDTA, pH 7.4). The cell suspension was homogenized on ice (Ultra-Turrax, 2 x 20 sec at full speed) and the homogenate was spun for 10 min (4 °C) at 3200 rpm. The

supernatant was centrifuged for 50 min at 37000 rpm at 4 °C. The membrane pellet was resuspended in the specific binding buffer ($hA_1$ ARs: 50 mM Tris/HCl buffer pH 7.4; $hA_{2A}$ ARs: 50 mM Tris/HCl, 50 mM $MgCl_2$ pH 7.4; $hA_3$ ARs: 50 mM Tris/HCl, 10 mM $MgCl_2$, 1 mM EDTA, pH 8.25), frozen in liquid nitrogen at a protein concentration of 2–4 mg/ml and stored at -80 °C.

*Radioligand binding*. Dissociation constants of radioligands ($K_D$ values) were obtained from saturation binding experiments. Dissociation constants of unlabelled compounds ($K_i$ values) were determined in radioligand competition experiments.

For saturation binding, increasing concentration of the radioligands [$^3$H]CCPA ([$^3$H]2-chloro-$N^6$–cyclopentyladenosine, $hA_1$ ARs), [$^3$H]NECA ([$^3$H]5'-N-ethylcarboxamidoadenosine, $hA_{2A}$ ARs), and [$^3$H]HEMADO ([$^3$H]2-(1-Hexynyl)-N-methyladenosine, $hA_3$ ARs) were incubated, in a 96-well plate, in a total volume of 200 µl containing 0.2 U/ml adenosine deaminase and 10 µg of membrane proteins in the specific buffer of each receptor.

In competition experiments, a fixed concentration of radioligand (1 nM [$^3$H]CCPA, $K_D$ = 1.1 nM; 10 nM [$^3$H]NECA, $K_D$ = 20 nM; [$^3$H] HEMADO, $K_D$ = 1.5 nM) was incubated in a 96-well plate with 10 µg of specific receptor-reach cell membranes and increasing concentrations of the compound understudy. Non-specific binding was determined in the presence of 1 mM theophylline for $hA_1$ AR and 100 µM (R)-$N^6$-phenyliso-propyladenosine (R-PIA) for both $hA_{2A}$ AR and $hA_3$ AR. Samples were incubated for 3 h at rt, filtered using a microplate format utilizing the 96-well microplate filtration system Microbeta Filtermat 96 Cell Harvester (PerkinElmer) to separate the free fractions to the bound fractions. The filters were washed three times with 200 µl of ice-cold binding buffer specific for each receptor and subsequently dried. After the addition of 20 µl of scintillation cocktail, the bound radioactivity was determined using a Perkin Elmer Microbeta$^2$ scintillation counter. All binding data were calculated by non-linear curve fitting with Prism 5.0 programme (GraphPAD Software, San Diego, CA, USA). Each concentration was tested three-five times in triplicate and the values are given as the mean ± standard error (S.E.). Radioligand binding at the $hA_{2B}$ AR is problematic because no high-affinity radioligand is commercially available for

this subtype. Therefore, inhibition of NECA-stimulated adenylyl cyclase was determined as a measurement of affinity of compounds.

*GloSensor cAMP Assay.* Cells, stably expressing the $hA_{2A}$ or $hA_{2B}$ AR and transiently the biosensor, were harvested in $CO_2$-independent medium and were counted in a Neubauer chamber. The desired number of cells was incubated in equilibration medium containing a 3% v/v GloSensor cAMP reagent stock solution, 10% FBS, and 87% $CO_2$ independent medium. After 2 h of incubation at rt, the cells were dispensed in the wells of a 384-well plate and, when a steady-state basal signal was obtained, the NECA reference agonist or the understudy compounds, at different concentrations, were added. When compounds were unable to stimulate the cAMP production they were studied as antagonists. In particular, the antagonist profile was evaluated by assessing the ability of these compounds to counteract NECA-induced increase of cAMP accumulation. The cells were incubated in the reaction medium (10 min at rt) with different understudy derivative concentrations and then treated with NECA. After 10 min, various luminescence measurements were performed at different incubation times.[64,65]

*Statistical analysis.* Responses were expressed as percentage of the maximal relative luminescence units (RLU). Concentration–response curves were fitted by a nonlinear regression with the Prism 5.0 programme (GraphPAD Software, San Diego, CA, USA). The antagonist profile of the two compounds was expressed as $IC_{50}$. The $IC_{50}$ value is the concentration of antagonists that produces 50% inhibition of the agonist effect. Each concentration was tested three-five times in triplicate and the values are given as the mean ± S.E.[66]

**SH-SY5Y cell assays**

*Cell culture.* Human neuroblastoma cell line (SH-SY5Y) was obtained from American Type Culture Collection (ATCC) and grown in DMEM medium supplemented with heat-inactivated FBS, including 1% penicillin and 1% streptomycin. Cells were grown in 10 $cm^2$ tissue culture dishes and cultured to a confluence of 80–90% and then subcultured with 0.25% trypsin. Cells were

maintained in a humidified atmosphere of 5% carbon dioxide ($CO_2$) at 37°C. The cell culture medium was replaced every 2 days. All the experiments were conducted at least three times.

*Cell treatments.* SH-SY5Y cells were seeded in 96-well plates at $8 \times 10^4$ cells in a final volume of 100 µl/well and incubated in a humidified atmosphere of 5% carbon dioxide ($CO_2$) at 37°C. Twenty-four hours after plating, cells were used for treatments. Cells were incubated for 24 h in the presence of $MPP^+$ at different concentrations, ranging from 50 µM to 3 mM. The dose that produces a significant neurotoxic effect was determined and used in the following neuroprotection experiments. Cells were incubated for 24 h in the presence of derivative **12** (0.5-30 nM) to demonstrate that this compound is not toxic. For neuroprotection experiments, cells were pretreated for 1 h with different concentrations of **12** (0.5-30 nM) and then with 1.5 mM $MPP^+$ for another 24 h. In addition, to evaluate the involvement of the $A_{2A}$ receptor, SH-SY5Y cells were treated with the $A_{2A}$ agonist **73** (10-100 nM) in presence of **12** (15 nM).

*Cell viability assay by CellTiter-Glo Luminescent.* The CellTiter-Glo® Luminescent Cell Viability Assay (Promega) is a homogeneous method to determine the number of viable cells in culture based on quantitation of the ATP present, which signals the presence of metabolically active cells. The addition of solution consisting of two reagents results in cell lysis and generation of a luminescent signal proportional to the amount of ATP present. The plates were equilibrated at rt for approximately 30 min. 100 µl of reagents were added to 100 µl of medium containing cells and incubated at rt for 10 min to stabilize luminescent signal. The luminescence is recorded with a luminometer.

*Data Analysis and Statistic*. Data, representative of three independent experiments, were expressed as means ± standard deviation (SD). One-way anova analysis of variance (ANOVA) followed by Tukey's test were used to compare differences between means in more than two groups. The level of significance was set at $P<0.01$. All the statistical analyses were performed with GraphPad Prism Software.

**Supporting information**

-Combustion analysis data of the newly synthesized compounds.

-Docking conformation of compound **10** at the $hA_1$ AR binding cavity.

-PDB coordinates of the 3D structures of the $hA_{2A}$ (PDB codes 3EML and 4EIY) and the $hA_1$ (PDB code 5UEN) adenosine receptors that were added of hydrogen atoms and missing loop segments and energetically minimized; PDB coordinates of the homology model of the $hA_3$ adenosine receptor based on the $hA_1$ receptor X-ray structure (PDB code 5UEN) as a template.

-SMILES data (CSV)

## AUTHOR INFORMATION

**Corresponding author**

*Tel: +39 055 4573731. e-mail: vittoria.colotta@unifi.it.

ORCID

Vittoria Colotta: 0000-0002-9296-6819

**ACKNOWLEDGMENTS**. The work was financially supported by the Italian Ministry for University and Research (MIUR, PRIN 2010-2011, 20103W4779_004 project), the University of Florence, and Ente Cassa di Risparmio di Firenze (2013.0664A2202.3926 project).

## ABBREVIATIONS USED

AR, adenosine receptor; MPTP, 1-methyl-4-phenyl-1,2,3,6-tetrahydropyridine; $MPP^+$, 1-methyl-4-phenyl-pyridinium; TQX, 1,2,4-triazolo[4,3-*a*]quinoxalin-1-one; CHO, chinese hamster ovary; mw, microwave; CCPA, 2-chloro-$N^6$–cyclopentyladenosine; NECA, 5'-(N-ethyl-carboxamido)adenosine; HEMADO, (2-(1-hexynyl)-N-methyladenosine; DMME, Dulbecco's modified Eagle's medium; FBS, fetal bovine serum; TM, transmembrane; EL, extracellular loop; MOE, molecular operating environment; RMS, root mean square

## REFERENCES


1. Fredholm, B. B.; IJzerman, A. P.; Jacobson, K. A.; Klotz, K.-N.; Linden, J. International union of Pharmacology XXV. Nomenclature and classification of adenosine receptors. *Pharmacol. Rev*. **2001**, *53*, 527-552
2. Fredholm, B. B.; IJzerman, A. P.; Jacobson, K. A.; Linden, J.; Muller, C. E. International union of Pharmacology LXXXI. Nomenclature and classification of adenosine receptors. An up date. *Pharmacol. Rev*. **2011**, *63*, 1-34.
3. Preti, D.; Baraldi, P. G.; Moorman, A. R.; Borea, P. A.; Varani, K. History and perspective of $A_{2A}$ adenosine receptor antagonists as potential therapeutic agents. *Med. Res. Rev.* **2015**, *35*, 790-848.
4. Martire, A.; Ferrante, A.; Potenza, R.L.; Armida, M.; Ferretti, R.; Pézzola, A.; Domenici, M. R.; Popoli, P. Remodeling of striatal NMDA receptors by chronic $A_{2A}$ receptor blockade in Huntington's disease mice. *Neurobiol. Dis.* **2010,** *37*, 99–105.
5. Li, W.; Silva, H. B.; Real, J.; Wang, Y.-M.; Rial, D.; Li, P.; Payen, M.-P.; Zhou, Y.; Muller, C. E.; Tomé, A. R.; Cunha, R. A.; Chen, J.-F. Inactivation of adenosine $A_{2A}$ receptors reverses working memory deficits at early stages of Huntington's disease models. *Neurobiol. Dis.* **2015**, *79*, 70–80.
6. Mohamed, R. A.; Agha, A. M.; Abdel-Rahman, A. A.; Nassar, N. N. Role of adenosine $A_{2A}$ receptor in cerebral ischemia reperfusion injury: signaling to phosphorylated extracellular signal-regulated protein kinase (pERK1/2). *Neuroscience* **2016**, *314*, 145–159.
7. Pedata, F.; Dettori, I.; Coppi, E.; Melani, A.; Fusco, I.; Corradetti, R.; Pugliese, A. M. Purinergic signalling in brain ischemia. *Neuropharmacology* **2016**, *104*, 105-130.
8. Navarro, G.; Borroto-Escuela, D. O.; Fuxe, K.; Franco, R. Purinergic signaling in Parkinson's disease. Relevance for treatment *Neuropharmacology* **2016**, *104*, 161-168.

9. Armentero, M. T.; Pinna, A.; Ferre, S.; Lanciego, J. L.; Muller, C. E.; Franco, R. Past, present and future of $A_{2A}$ adenosine receptor antagonists in the therapy of Parkinson's disease. *Pharmacol. Ther.* **2011**, *132*, 280–299.

10. Kyowa Hakko Kirin, Approval for manufacturing and Marketing of NOURIAST tablets 20 mg. A novel Antiparkinsonian Agent, http://www.kyowa-kirin.com/news_releases/2013/e20130529_01.html May 29, 2013.

11. Ferre, S.; von Euler, G.; Johansson, B.; Fredholm, B. B.; Fuxe, K. Stimulation of high-affinity adenosine $A_2$ receptors decreases the affinity of dopamine $D_2$ receptors in rat striatal membranes. *Proc. Natl. Acad. Sci. U.S.A.* **1991**, *88*, 7238-7241.

12. Fuxe, K.; Franco, R.; Agnati, L. F. Adenosine receptor–dopamine receptor interactions in the basal ganglia and their relevance for brain function. *Physiol. Behav.* **2007**, *92*, 210–217.

13. Orru, M.; Bakesˇova´, J.; Brugarolas, M.; Quiroz, C.; Beaumont, V.; Goldberg, S. R.; Carme Lluı´s, C.; Cortes, A.; Franco, R.; Casado´, V.; Canela, E. I.; Ferrè, S. Striatal pre- and postsynaptic profile of adenosine $A_{2A}$ receptor antagonists, *PLoS One* **2011**, *6*, e16088.

14. Yamada, K.; Kobayashi, M.; Shiozaki, S.; Ohta, T.; Mori, A.; Jenner, P.; Kanda, T. Antidepressant activity of the adenosine $A_{2A}$ receptor antagonist, istradefylline (KW-6002) on learned helplessness in rats. *Psychopharmacology* **2014**, *231*, 2839–2849.

15. Horita, T. K.; Kobayashi, M.; Mori, A.; Jenner, P.; Kanda, T. Effects of the adenosine $A_{2A}$ antagonist istradefylline on cognitive performance in rats with a 6-OHDA lesion in prefrontal cortex. *Psychopharmacology* **2013**, *230*, 345-352.

16. Ikeda, K.; Kurokawa, M.; Aoyama, S.; Kuwana, Y. Neuroprotection by adenosine $A_{2A}$ receptor blockade in experimental models of Parkinson's disease. *J. Neurochem.* **2002**, *80*, 262–270.

17. Yu, L.; Shen, H. Y.; Coelho, J. E.; Araujo, I. M.; Huang, Q. Y.; Day, Y.-J.; Rebola, N.; Canas, P. N.; Rapp, E. K.; Ferrara, J.; Taylor, D.; Müller, C. E.; Linden, J.; Cunha R. A.;

Chen, J.-F. Adenosine $A_{2A}$ receptor antagonists exert motor and neuroprotective effects by distinct cellular mechanisms. *Ann. Neurol.* **2008**, *63*, 338–346.

18. Carta, A. R.; Kachroo, A.; Schintu, N.; Xu, K.; Schwarzschild, M. A.; Wardas, J.; Morelli, M. Inactivation of neuronal forebrain A receptors protects dopaminergic neurons in a mouse model of Parkinson's disease. *J. Neurochem.* **2009**, *111*, 1478–1489.
19. Gyoneva, S.; Shapiro, L.; Lazo, C.; Garnier-Amblard, E.; Smith, Y.; Miller, G. W.; Traynelis, S. F. Adenosine $A_{2A}$ receptor antagonism reverses inflammation-induced impairment of microglial process extension in a model of Parkinson's disease. *Neurobiol. Dis.* **2014**, *67*, 191-202.
20. Poli, D.; Catarzi D.; Colotta V.; Varano, F.; Filacchioni, G.; Daniele, S.; Trincavelli, L.; Martini, C.; Paoletta, S.; Moro, S. The identification of the 2-phenylphthalazin-1(2H)-one scaffold as a new decorable core skeleton for the design of potent and selective human $A_3$ adenosine receptor antagonists. *J. Med. Chem*. **2011**, *54*, 2102-2113.
21. Squarcialupi, L.; Colotta, V.; Catarzi, D.; Varano, F.; Filacchioni, G.; Varani, K.; Corciulo, C.; Vincenzi, F.; Borea, P. A.; Ghelardini, C.; Di Cesare Mannelli, L.; Ciancetta, A.; Moro, S. 2-Arylpyrazolo[4,3-*d*]pyrimidin-7-amino derivatives as new potent and selective human $A_3$ adenosine receptor antagonists. Molecular modeling studies and pharmacological evaluation. *J. Med. Chem*. **2013**, *56*, 2256-2269.
22. Squarcialupi, L.; Colotta, V.; Catarzi, D.; Varano, F.; Betti, M.; Varani, K.; Vincenzi, F.; Borea, P. A.; Porta, N.; Ciancetta, A.; Moro, S. 7-Amino-2-phenylpyrazolo[4,3-*d*]pyrimidine derivatives: structural investigations at the 5-position to target $A_1$ and $A_{2A}$ adenosine receptors. Molecular modeling and pharmacological studies. *Eur. J. Med. Chem*. **2014**, *84*, 614-627.
23. Squarcialupi, L.; Falsini, M.; Catarzi, D.; Varano, F.; Betti, M.; Varani, K.; Vincenzi, F.; Dal Ben, D.; Lambertucci, C.; Volpini, R.; Colotta, V. Exploring the 2- and 5-positions of the

pyrazolo[4,3-*d*]pyrimidin-7-amino scaffold to target human $A_1$ and $A_{2A}$ adenosine receptors. *Bioorg. Med. Chem*. **2016**, *24,* 2794-2808.

24. Varano, F.; Catarzi D.; Vincenzi, F.; Betti, M.; Falsini, M.; Ravani, A.;Borea, P. A.; Colotta, V.; Varani, K. Design, synthesis, and pharmacological characterization of 2-(2-furanyl)thiazolo[5,4-*d*]pyrimidine-5,7-diamine derivatives: New highly potent $A_{2A}$ adenosine receptor inverse agonists with antinociceptive activity. *J. Med. Chem*. **2016**, *59*, 10564-10576.
25. Squarcialupi, L.; Betti, M.; Catarzi, D.; Varano, F.; Falsini, M.; Ravani, A.; Pasquini, S.; Vincenzi, F.; Salmaso, V.; Sturlese, M.; Varani, K.; Moro, S.; Colotta V. The role of 5-arylalkylamino- and 5-piperazino- moieties on the 7-aminopyrazolo[4,3-*d*]pyrimidine core in affecting adenosine $A_1$ and $A_{2A}$ receptor affinity and selectivity profiles. *J. Enzyme Inhib. Med. Chem.* **2017***, 32,* 248-263.
26. Colotta, V.; Catarzi, D.; Varano, F.; Cecchi, L.; Filacchioni, G.; Martini, C.; Trincavelli, L.; Lucacchini, A. Synthesis and structure-activity relationships of a new sets of 2-arylpyrazolo[3,4-*c*]quinoline derivatives as adenosine receptor antagonists. *J. Med. Chem.* **2000**, *43*, 3118-3124.
27. Lenzi, O., Colotta, V.; Catarzi, D.; Varano, F.; Squarcialupi, L.; Filacchioni, G.; Varani, K.; Vincenzi, F.; Borea, P. A.; Dal Ben, D.; Lambertucci, C.; Cristalli, G. Synthesis, structure-affinity relationships and molecular modeling studies of novel pyrazolo[3,4-*c*]quinoline derivatives as adenosine receptor antagonists. *Bioorg. Med. Chem*. **2011**, *19*, 3757-3768.
28. Colotta, V.; Catarzi, D.; Varano, F.; Calabri, F. R.; Lenzi, O.; Filacchioni, G.; Trincavelli, L.; Martini, C.; Deflorian, F.; Moro S. 1,2,4-Triazolo[4,3-*a*]quinoxalin-1-one moiety as an attractive scaffold to develop new potent and selective human $A_3$ adenosine receptor antagonists: synthesis, pharmacological and ligand-receptor modeling studies. *J. Med. Chem.* **2004**, *47*, 3580-3590.

29. Colotta, V.; Catarzi, D.; Varano, F.; Filacchioni, G.; Martini, C.; Trincavelli, L.; Lucacchini, A. Synthesis of 4-Amino-6-(hetero)arylalkylamino-1,2,4-triazolo[4,3-*a*]quinoxalin-1-one derivative as potent $A_{2A}$ adenosine receptor antagonists. *Bioorg. Med. Chem.* **2003**, *11,* 5509-5518.

30. Lenzi, O.; Colotta, V.; Catarzi, D.; Varano, F.; Filacchioni, G.; Martini, C.; Trincavelli, L.; Ciampi, O.; Marighetti, F.; Morizzo, E.; Moro S. 4-Amido-2-aryl-1,2,4-triazolo[4,3-*a*]quinoxalin-1-ones as new potent and selective human $A_3$ adenosine receptor antagonists. Synthesis, pharmacological evaluation and ligand-receptor modeling studies. *J. Med. Chem.* **2006**, *49*, 3916-3925.

31. Morizzo, E.; Capelli, F.; Lenzi, O.; Catarzi, D.; Varano, F.; Filacchioni, G.; Vincenzi, F.; Varani, K.; Borea, P. A.; Colotta, V.; Moro, S. Scouting human $A_3$ adenosine receptor antagonist binding mode using a molecular simplification approach: from triazoloquinoxaline to a pyrimidine skeleton as a key study. *J. Med. Chem.* **2007**, *50,* 6596-6606.

32. Colotta, V.; Catarzi, D.; Varano, F.; Lenzi, O.; Filacchioni, G.; Martini, C.; Trincavelli, L.; Ciampi, O.; Traini, C.; Pugliese, A. M.; Pedata, F.; Morizzo, E.; Moro, S. Synthesis, ligand-receptor modeling studies and pharmacological evaluation of novel 4-modified-2-aryl-1,2,4-triazolo[4,3-*a*]quinoxalin-1-one derivatives as potent and selective human $A_3$ Adenosine Receptor Antagonists. *Bioorg. Med. Chem.* **2008**, *16,* 6086-6102.

33. Shawali, A. S.; Albar, H. A. Kinetics and mechanism of dehydrochlorination of *N*-aryl-*C*-ethoxycarbonylformohydrazidoyl chlorides. *Can. J. Chem*. **1986**, *64*, 871-875.

34. Lozinskii, M. O.; Kukota, S. N.; Pel'kis, P. S. Ethyl arylazochloroacetates and their reactions with morpholine and hydrazine hydrate. *Ukr. Khim. Zh*. **1967**, *33*, 1295-1296.

35. Abbotto, A.; Bradamante, S.; Facchetti, A.; Pagani, G. A. Diheteroarylmethanes. 8.1 Mapping charge and electron-withdrawing power of the 1,2,4-triazol-5-yl substituent. *J. Org. Chem*. **1999**, *64,* 6756-6763.

36. Sharp, D. B.; Hamilton C. S. Derivatives of 1,2,4-triazole and pyrazole. *J. Am. Chem. Soc*. **1946**, *68*, 588-590.

37. Matiychuk, V. S.; Potopnyk, M. A.; Luboradzki, R.; Obushak, M. D. A New method for the synthesis of 1-aryl-1,2,4-triazole derivatives. *Synthesis* **2011**, *11*, 1799–1803.

38. Scatena, A.; Fornai, F.; Trincavelli, M. L.; Taliani, S.; Daniele, S.; Pugliesi, I.; Cosconati, S.; Martini, C.; Da Settimo, F. 3-(Fur-2-yl)-10-(2-phenylethyl)-[1,2,4]triazino[4,3-*a*]benzimidazol-4(10H)-one, a novel adenosine receptor antagonist with $A_{2A}$-mediated neuroprotective effects. *ACS Chem. Neurosci*. **2011**, *2*, 526-535.

39. Zhao, Q.; Ye, J.; Wei, N.; Fong, C.; Dong, X. Protection against $MPP^+$-induced neurotoxicity in SH-SY5Y cells by tormentic acid via the activation of PI3-K/Akt/GSK3 pathway. *Neurochem. Int*. **2016**, *97*, 117-123.

40. Maatougui, A. E.; Azuaje, J.; González-Gómez, M.; Miguez, G.; Crespo, A.; Carbajales, C.; Escalante, L.; García-Mera, X.; Gutiérrez-de-Terán, H.; Sotelo, E. Discovery of potent and highly selective $A2_B$ adenosine receptor antagonist chemotypes. *J. Med. Chem.* **2016**, *59*, 1967-1983.

41. Alnouri, M. W.; Jepards, S.; Casari, A.; Schiedel, A. C.; Hinz, S.; Müller, C. E. Selectivity is species-dependent: Characterization of standard agonists and antagonists at human, rat, and mouse adenosine receptors. *Purinergic Signalling* **2015**, *11*, 389-407.

42. Maemoto, T.; Tada, M.; Mihara, T.; Ueyama, N.; Matsuoka, H.; Harada, K.; Yamaji, T.; Shirakawa, J.; Kuroda, S.; Akahane, A.; Iwashita, A.; Matsuoka, N.; Mutoh, S. Pharmacological characterization of FR194921, a new potent, selective, and orally active antagonist for central adenosine $A_1$ receptors. *J. Pharmacol. Sci.* **2004**, *96,* 42-52.

43. Mihara, T.; Iwashita, A.; Matsuoka, N. A novel adenosine $A_1$ and $A_{2A}$ receptor antagonist ASP5854 ameliorates motor impairment in MPTP-treated marmosets: comparison with existing anti-Parkinson's disease drugs. *Behav. Brain Res*. **2008**, *194,* 152-161.

44. Atack J. R.; Shook, B. C.; Rassnick, S.; Jackson, P. F.; Rhodes, K.; Drinkenburg, W. H.; Ahnaou, A.; Te Riele, P.; Langlois, X.; Hrupka, B.; De Haes, P.; Hendrickx, H.; Aerts, N.; Hens, K.; Wellens, A.; Vermeire, J.; Megens, A. A. JNJ-40255293, a novel adenosine $A_{2A}/A_1$ antagonist with efficacy in preclinical models of Parkinson's disease. *ACS Chem. Neurosci*. **2014**, *5*, 1005-1019.

45. Checova, S.; Elsobky, A. M.; Venton, B. J. $A_1$ receptors self-regulate adenosine release in the striatum: evidence of autoreceptor characteristics. *Cell. Mol. Neurosci.* **2010**, *171*, 1006-1015.

46. Borycz, J.; Pereira, M. -F.; Melani, A.; Rodriguez, R. -J.; Kofalvi, A.; Panlilio, L.; Pedata, F.; Goldberg, S. -R.; Cunha, R. -A.; Ferré, S. Differential glutamate-dependent and glutamate independent adenosine $A_1$ receptor-mediated modulation of dopamine release in different striatal compartments. *J. Neurochem*. **2007**, *101*, 355-363.

47. Fahn, S. Description of Parkinson's disease as a clinical syndrome. *Ann. N. Y. Acad. Sci*. **2003**, *991*, 1-14.

48. Blum, D.; Torch, S.; Lambeng, N.; Nissou, M.; Benabid, A. L.; Sadoul, R.; Verna, J. -M. Molecular pathways involved in the neurotoxicity of 6-OHDA, dopamine and MPTP: contribution to the apoptotic theory in Parkinson's disease. *Prog. Neurobiol*. **2001**, *65*, 135-172.

49. Caulkett, P. W. R.; Jones, G.; Collis, M. G.; Poucher, S. M. Preparation of (Amino)heteroaryl[1,2,4]triazolo[1,5-a]triazine and related compounds as adenosine A2 receptor antagonists. EP 459702, May 23, 1991.

50. Hutchison, A. J.; Webb, R. L.; Oei, H. H.; Ghai, G. R.; Zimmerman, M. B.; Williams, M. CGS21680, an A2 selective adenosine receptor agonist with preferential hypotensive activity. *J. Pharm. Exp. Ther.* **1989**, *251*, 47-55.

51. *Molecular Operating Environment*, 2014, C.C.G., Inc., 1255 University St., Suite 1600, Montreal, Quebec, Canada, H3B 3X3.

52. Jones, G.; Willett, P.; Glen, R. C.; Leach, A. R.; Taylor, R. Development and validation of a genetic algorithm for flexible docking. *J. Mol. Biol.* **1997**, *267*, 727-748.

53. Huey, R.; Morris, G. M.; Olson, A. J.; Goodsell, D. S. A semiempirical free energy force field with charge-based desolvation. *J. Comput. Chem.* **2007**, *28*, 1145-1152.

54. Morris, G. M.; Huey, R.; Lindstrom, W.; Sanner, M. F.; Belew, R. K.; Goodsell, D. S.; Olson, A. J. AutoDock4 and AutoDockTools4: Automated docking with selective receptor flexibility. *J. Comput. Chem.* **2009**, *30*, 2785-2791.

55. Jaakola, V. P.; Griffith, M. T.; Hanson, M. A.; Cherezov, V.; Chien, E. Y.; Lane, J. R.; IJzerman, A. P.; Stevens, R. C. The 2.6 angstrom crystal structure of a human $A_{2A}$ adenosine receptor bound to an antagonist. *Science* **2008**, *322*, 1211-1217.

56. Dal Ben, D.; Lambertucci, C.; Marucci, G.; Volpini, R.; Cristalli, G. Adenosine receptor modeling: what does the $A_{2A}$ crystal structure tell us? *Curr. Top. Med. Chem.* **2010**, *10*, 993-1018.

57. Liu, W.; Chun, E.; Thompson, A. A.; Chubukov, P.; Xu, F.; Katritch, V.; Han, G. W.; Roth, C. B.; Heitman, L. H.; IJzerman, A. P.; Cherezov, V.; Stevens, R. C. Structural basis for allosteric regulation of GPCRs by sodium ions. *Science* **2012**, *337*, 232-236.

58. Glukhova, A.; Thal, D.M.; Nguyen AT, Vecchio EA, Jörg M, Scammells PJ, May LT, Sexton PM, Christopoulos A. Structure of the adenosine $A_1$ receptor reveals the basis for subtype selectivity. *Cell* **2017**, *168*, 867-877 e13.

59. Dal Ben, D.; Buccioni, M.; Lambertucci, C.; Marucci, G.; Thomas, A.; Volpini, R.; Cristalli, G. Molecular modeling study on potent and selective adenosine $A_3$ receptor agonists. *Bioorg. Med. Chem.* **2010**, *18*, 7923-7930.

60. Dal Ben, D.; Buccioni, M.; Lambertucci, C.; Thomas, A.; Volpini, R. Simulation and comparative analysis of binding modes of nucleoside and non-nucleoside agonists at the $A_{2B}$ adenosine receptor. *In Silico Pharmacol.* **2013**, *1*, 24.

61. Varano, F.; Catarzi, D.; Squarcialupi, L.; Betti, M.; Vincenzi, F.; Ravani, A.; Varani, K.; Dal Ben, D.; Thomas, A.; Volpini, R.; Colotta, V. Exploring the 7-oxo-thiazolo[5,4-*d*]pyrimidine core for the design of new human adenosine $A_3$ receptor antagonists. Synthesis, molecular modeling studies and pharmacological evaluation. *Eur. J. Med. Chem.* **2015**, *96*, 105-121.

62. Dal Ben, D.; Buccioni, M.; Lambertucci, C.; Marucci, G.; Santinelli, C.; Spinaci, A.; Thomas, A.; Volpini, R. Simulation and comparative analysis of different binding modes of non-nucleoside agonists at the $A_{2A}$ adenosine receptor. *Mol. Inf.* **2016**, *35*, 403-413.

63. Dallakyan, S.; Olson, A. J. Small-molecule library screening by docking with PyRx. *Methods Mol. Biol.* **2015**, *1263*, 243-250.

64. Thomas, A.; Buccioni, M.; Dal Ben, D.; Lambertucci, C.; Marucci, G.; Santinelli, C.; Spinaci, A.; Kachler, S.; Klotz, K.- N.; Volpini, R. The length and flexibility of the 2-substituent of 9-ethyladenine derivatives modulate affinity and selectivity for the human $A_{2A}$ adenosine receptor, *ChemMedChem* **2016**, *11*, 1829-1839.

65. Buccioni, M.; Santinelli, C.; Angeli, P.; Dal Ben, D.; Lambertucci, C.; Thomas, A.; Volpini, R.; Marucci, G. Overview on radiolabel-free in vitro assays for GPCRs. *Mini Rev. Med. Chem*. **2017**, *17*, 3-14.

66. Buccioni, M.; Marucci, G.; Dal Ben, D.; Giacobbe, D.; Lambertucci, C.; Soverchia, L.; Thomas, A.; Volpini, R.; Cristalli, G. Innovative functional cAMP assay for studying G protein-coupled receptors: application to the pharmacological characterization of GPR17. *Purinergic Signalling* **2011**, *7*, 463-468.

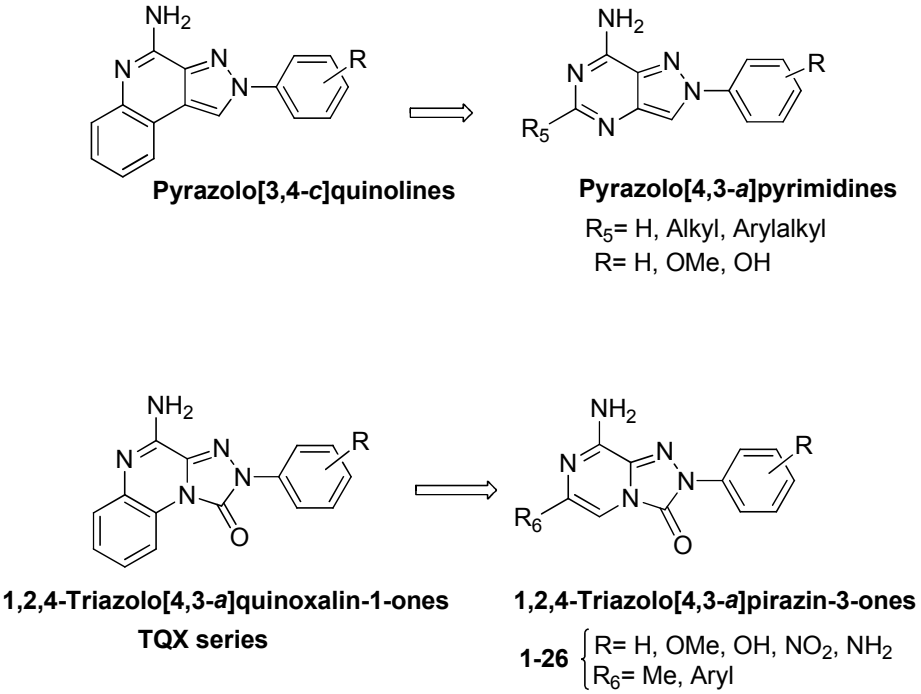


**Chart 1**. A structural modification approach to develop new $hA_{2A}$ AR antagonists: from tricyclic to bicyclic chemotypes.

**Scheme 1**

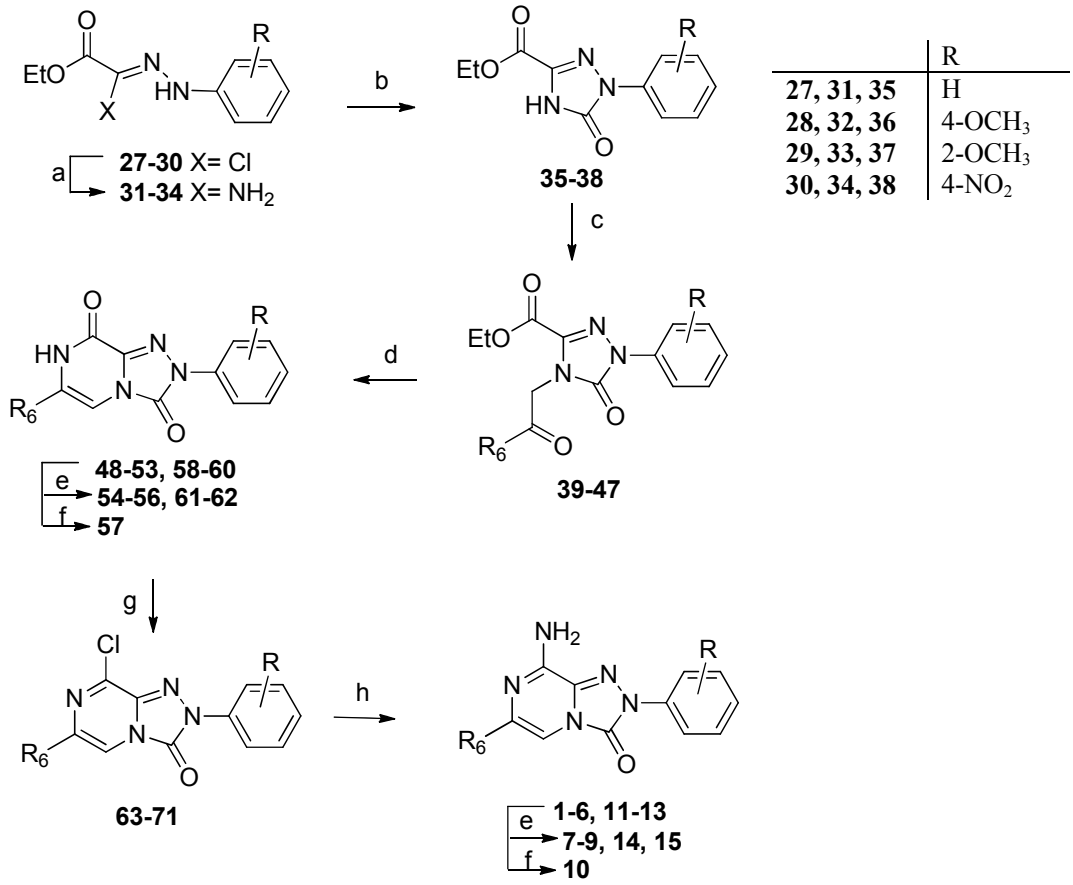


| | R |
|---|---|
| **27, 31, 35** | H |
| **28, 32, 36** | 4-$OCH_3$ |
| **29, 33, 37** | 2-$OCH_3$ |
| **30, 34, 38** | 4-$NO_2$ |

| | $R_6$ | R | | $R_6$ | R |
|---|---|---|---|---|---|
| **1, 39, 48, 63** | $CH_3$ | H | **9, 56** | $C_6H_5$ | 2-OH |
| **2, 40, 49, 64** | $C_6H_5$ | H | **10, 57** | $C_6H_5$ | 4-$NH_2$ |
| **3, 41, 50, 65** | $CH_3$ | 4-$OCH_3$ | **11, 45, 58, 69** | $C_6H_4$-3-$OCH_3$ | H |
| **4, 42, 51, 66** | $C_6H_5$ | 4-$OCH_3$ | **12, 46, 59, 70** | $C_6H_4$-4-$OCH_3$ | H |
| **5, 43, 52, 67** | $C_6H_5$ | 4-$NO_2$ | **13, 47, 60, 71** | $C_6H_4$-4-$CH_3$ | H |
| **6, 44, 53, 68** | $C_6H_5$ | 2-$OCH_3$ | **14, 61** | $C_6H_4$-3-OH | H |
| **7, 54** | $CH_3$ | 4-OH | **15, 62** | $C_6H_4$-4-OH | H |
| **8, 55** | $C_6H_5$ | 4-OH | | | |

Reagents and conditions: (a) 33% aqueous $NH_3$, 1,4-dioxane, rt; (b) triphosgene, anhydrous THF, rt; (c) $CH_3COCH_2Cl$ or Ar-$COCH_2Br$, $K_2CO_3$, DMF/$CH_3CN$, rt; (d) $NH_4OAc$, mw or conventional heating, 130-190 °C; (e) $BBr_3$, anhydrous $CH_2Cl_2$, 0 °C to rt, or 48% HBr, AcOH, reflux; (f) $H_2$, Pd/C, DMF, Parr apparatus, 40 psi; (g) $POCl_3$, mw or conventional heating, 140-180 °C; (h) $NH_3$/absolute EtOH.

**Scheme 2**

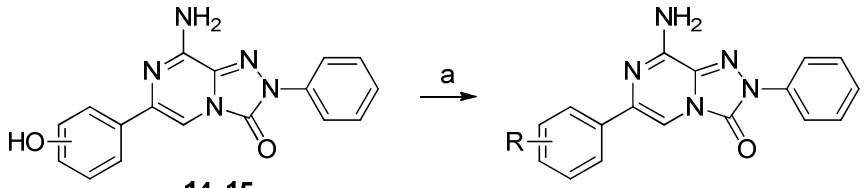


**14, 15** **16-26**

| | R |
|---|---|
| **16** | 3-OPropargyl |
| **17** | 4-OPropargyl |
| **18** | 3-$OCH_2$-$C_6H_5$ |
| **19** | 4-$OCH_2$-$C_6H_5$ |
| **20** | 4-$OC_2H_5$ |
| **21** | 4-O-n$C_3H_7$ |
| **22** | 4-O-i$C_3H_7$ |
| **23** | 4-$OCH_2$-i$C_3H_7$ |
| **24** | 4-$OCH_2$c$C_3H_5$ |
| **25** | 4-$OCH_2$c$C_4H_7$ |
| **26** | 4-$OCH_2$-CH=$CH_2$ |

Reagents and conditions: (a) suitable alkylbromide, $K_2CO_3$, 2-butanone, reflux.

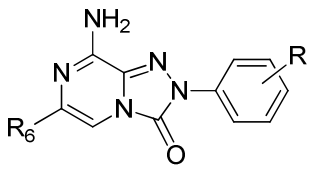


**Table 1.** Biological activity of compounds **1-26** and reference ligands at hARs[a]

| | | | Binding experiments $K_i$ (nM) or I% | | | cAMP assays $IC_{50}$ (nM) |
|---|---|---|---|---|---|---|
| | $R_6$ | R | $hA_1$[b] | $hA_{2A}$[c] | $hA_3$[d] | $hA_{2B}$[e] |
| **1** | $CH_3$ | H | 67 ± 8 | 485 ± 39 | 4370 ± 355 | > 30000 |
| **2** | $C_6H_5$ | H | 13 ± 1 | 10 ± 3 | 11 ± 2 | > 30000 |
| **3** | $CH_3$ | 4-$OCH_3$ | 1743 ± 514 | 1038 ± 271 | 255 ± 21 | > 30000 |
| **4** | $C_6H_5$ | 4-$OCH_3$ | 20 ± 5 | 78 ± 18 | 117 ± 26 | > 30000 |
| **5** | $C_6H_5$ | 4-$NO_2$ | 8.1 ± 2.5 | 402 ± 91 | > 30000 | > 30000 |
| **6** | $C_6H_5$ | 2-$OCH_3$ | 247 ± 31 | 309 ± 37 | 392 ± 60 | > 30000 |
| **7** | $CH_3$ | 4-OH | 1000 ± 128 | 1319 ± 184 | 5159 ± 752 | > 30000 |
| **8** | $C_6H_5$ | 4-OH | 18 ± 2 | 138 ± 28 | 429 ± 89 | > 30000 |
| **9** | $C_6H_5$ | 2-OH | 47 ± 9 | 232 ± 47 | 1558 ± 393 | > 30000 |
| **10** | $C_6H_5$ | 4-$NH_2$ | 8.9 ± 1.1 | 3480 ± 398 | 650 ± 143 | > 30000 |
| **11** | $C_6H_4$-3-$OCH_3$ | H | 44 ± 7 | 6.8 ± 0.7 | 42 ± 10 | > 30000 |
| **12** | $C_6H_4$-4-$OCH_3$ | H | > 30000 | 7.2 ± 1.8 (180 ± 34)[f] | > 30000 | > 30000 |
| **13** | $C_6H_4$-4-$CH_3$ | H | > 30000 | > 30000 | >30000 | > 30000 |
| **14** | $C_6H_4$-3-OH | H | 14 ± 2 | 3.5 ± 0.6 | 134 ± 13 | > 30000 |
| **15** | $C_6H_4$-4-OH | H | 45 ± 10 | 45 ± 12 | 53 ± 13 | > 30000 |
| **16** | $C_6H_4$-3-OPropargyl | H | 45 ± 10 | 5.1 ± 1.5 | 67 ± 9 | > 30000 |
| **17** | $C_6H_4$-4-OPropargyl | H | > 30000 | 10.6 ± 1.3 | > 30000 | > 30000 |
| **18** | $C_6H_4$-3-$OCH_2Ph$ | H | > 30000 | > 30000 | > 30000 | > 30000 |
| **19** | $C_6H_4$-4-$OCH_2Ph$ | H | 3704 ± 495 | 708 ± 160 | > 30000 | > 30000 |
| **20** | $C_6H_4$-4-$OC_2H_5$ | H | > 30000 | 2.9 ± 0.5 (98 ± 19)[f] | > 30000 | > 30000 |
| **21** | $C_6H_4$-4-O-n$C_3H_7$ | H | > 30000 | Nd[g] | > 30000 | > 30000 |
| **22** | $C_6H_4$-4-O-i$C_3H_7$ | H | > 30000 | 7.4 ± 0.9 | > 30000 | > 30000 |
| **23** | $C_6H_4$-4-$OCH_2$-i$C_3H_7$ | H | Nd[g] | Nd[g] | Nd[g] | Nd[g] |
| **24** | $C_6H_4$-4-$OCH_2$c$C_3H_5$ | H | > 30000 | > 30000 | > 30000 | > 30000 |
| **25** | $C_6H_4$-4-$OCH_2$c$C_4H_7$ | H | > 30000 | > 30000 | > 30000 | > 30000 |
| **26** | $C_6H_4$-4-$OCH_2$-CH=$CH_2$ | H | Nd[g] | Nd[g] | Nd[g] | Nd[g] |
| | DPCPX | | 2.8 ± 0.5 | 125 ± 21 | 3850 ± 762 | 989 ± 22 |

| | | | | |
|---|---|---|---|---|
| | | | | (73.24 ± 2.0)[h] |
| NECA | 4.6 ± 0.8 | 16 ± 3 | 12.8 ± 2.5 | 1510 ± 210[i] (1890)[h] |
| CCPA | 1.2 ± 0.2 | 2050 ± 400 | 26 ± 5 | 16850 ± 320[i] (18800)[h] |

[a]Data (n= 3-5) are expressed as means ± standard errors. [b]Displacement of specific [$^3$H]-CCPA binding at $hA_1$ AR expressed in CHO cells. [c]Displacement of specific [$^3$H]-NECA binding at $hA_{2A}$ AR expressed in CHO cells. [d]Displacement of specific [$^3$H]-HEMADO binding at $hA_3$ AR expressed in CHO cells. [e]$IC_{50}$ values of the inhibition of NECA-stimulated adenylyl cyclase activity in CHO cells expressing $hA_{2B}$ AR. [f]$IC_{50}$ values of the inhibition of NECA-stimulated adenylyl cyclase activity in CHO cells expressing $hA_{2A}$ AR. [g]Not determined. [h]$K_i$ values (nM) from radioligand binding assays, ref. 40 for DPCPX, ref. 41 for NECA and CCPA. [i]$EC_{50}$ value (nM) of the stimulation of adenylyl cyclase activity in CHO cells expressing $hA_{2B}$ AR.

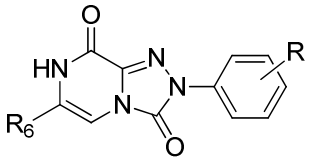

**Table 2** Biological activity of compounds **48-62** and reference ligands at hARs[a]

| | | | Binding experiments $K_i$ (nM) or I% | | | cAMP assays $IC_{50}$ (nM) |
|---|---|---|---|---|---|---|
| | $R_6$ | R | $hA_1$[b] | $hA_{2A}$[c] | $hA_3$[d] | $hA_{2B}$[e] |
| **48** | $CH_3$ | H | > 30000 | > 30000 | 60 ± 5 | > 30000 |
| **49** | $C_6H_5$ | H | > 30000 | > 30000 | 96 ± 15 | > 30000 |
| **50** | $CH_3$ | 4-$OCH_3$ | > 30000 | > 30000 | 50 ± 12 | > 30000 |
| **51** | $C_6H_5$ | 4-$OCH_3$ | > 30000 | > 30000 | 214 ± 54 | > 30000 |
| **52** | $C_6H_5$ | 4-$NO_2$ | Nd[f] | Nd[f] | Nd[f] | Nd[f] |
| **53** | $C_6H_5$ | 2-$OCH_3$ | 2142 ± 526 | > 30000 | 5200 ± 927 | > 30000 |
| **54** | $CH_3$ | 4-OH | 5740 ± 1241 | Nd[f] | 229 ± 69 | > 30000 |
| **55** | $C_6H_5$ | 4-OH | 129 ± 27 | 387 ± 36 | 0.37 ± 0.06 | > 30000 |
| **56** | $C_6H_5$ | 2-OH | 1480 ± 259 | > 30000 | 21600 ± 5030 | > 30000 |
| **57** | $C_6H_5$ | 4-$NH_2$ | 247 ± 56 | 415 ± 25 | 63 ± 2 | > 30000 |
| **58** | $C_6H_4$-3-$OCH_3$ | H | > 30000 | > 30000 | > 30000 | > 30000 |
| **59** | $C_6H_4$-4-$OCH_3$ | H | > 30000 | > 30000 | > 30000 | > 30000 |
| **60** | $C_6H_4$-4-$CH_3$ | H | > 30000 | > 30000 | > 30000 | > 30000 |
| **61** | $C_6H_4$-3-OH | H | 698 ± 114 | 4066 ± 909 | 1054 ± 295 | > 30000 |
| **62** | $C_6H_4$-4-OH | H | 616 ± 166 | > 30000 | 207 ± 82 | > 30000 |
| | DPCPX | | 2.8 ± 0.5 | 125 ± 21 | 3850 ± 762 | 989 ± 22 (73.24 ± 2.0)[g] |
| | NECA | | 4.6 ± 0.8 | 16 ± 3 | 12.8 ± 2.5 | 1510 ± 210[h] (1890)[g] |
| | CCPA | | 1.2 ± 0.2 | 2050 ± 400 | 26 ± 5 | 16850 ± 320[h] (18800)[g] |

[a]Data (n= 3-5) are expressed as means ± standard errors. [b]Displacement of specific [$^3$H]-CCPA binding at $hA_1R$ expressed in CHO cells. [c]Displacement of specific [$^3$H]-NECA binding at $hA_{2A}R$ expressed in CHO cells. [d]Displacement of specific [$^3$H]-HEMADO binding at $hA_3R$ expressed in CHO cells. [e]$IC_{50}$ values of the inhibition of NECA-stimulated adenylyl cyclase activity in CHO cells expressing $hA_{2B}R$. [f]Not determined. [g]$K_i$ values (nM) from radioligand binding assays, ref. 40 for DPCPX, ref. 41 for NECA and CCPA. [h]$EC_{50}$ value (nM) of the stimulation of adenylyl cyclase activity in CHO cells expressing $hA_{2B}$ AR.

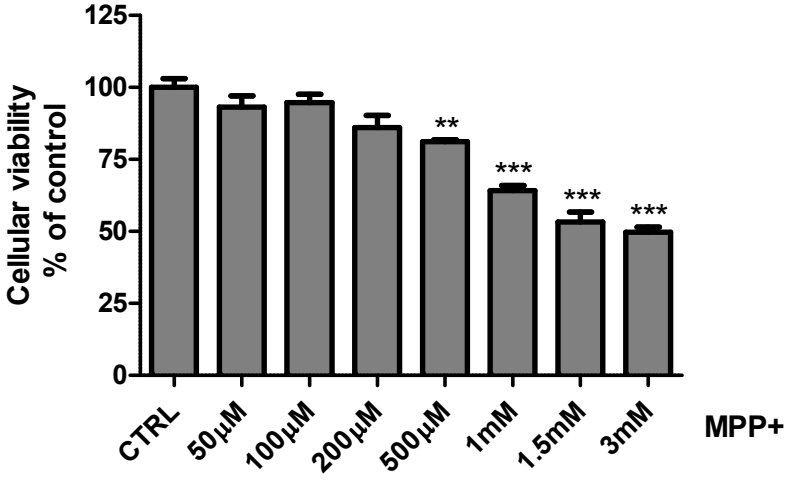


**Figure 1.** Dose-dependency of $MPP^+$ in SH-SY5Y cells. Cellular viability was carried out after 24 h of $MPP^+$. Effect of $MPP^+$ on cell viability was measured by CellTiter-Glo® Luminescent assay. Data are expressed as mean of three independent experiments. **P <0.01 compared with control; ***P <0.001 compared with control.

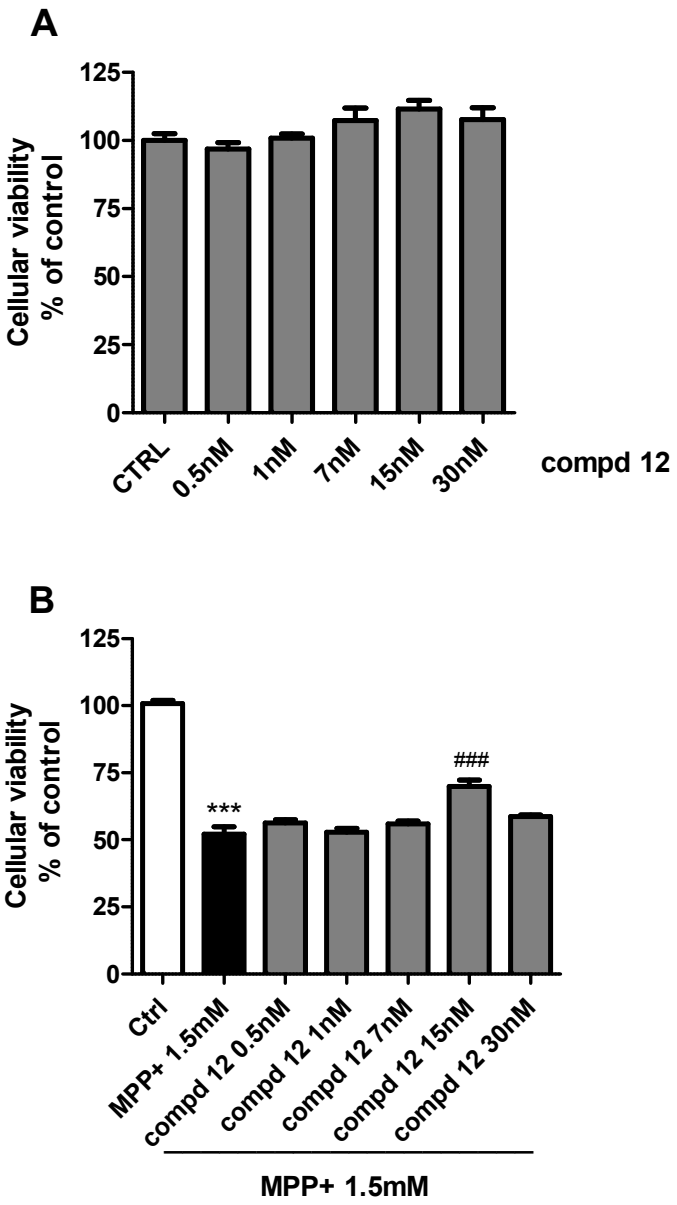


**Figure 2.** SH-SY5Y cells were treated for 24 h with different concentrations of compound **12** from 0.5 to 30 nM, alone (panel A) and in presence of $MPP^+$ 1.5 mM (panel B). Compound **12** proved not to be toxic and neuroprotective against $MPP^+$ in SH-SY5Y cells after CellTiter-Glo® luminescent cell-viability assay. Data are expressed as mean of three independent experiments. ***P<0.001 compared with control, ###P<0.001 compared to $MPP^+$ 1.5 mM.

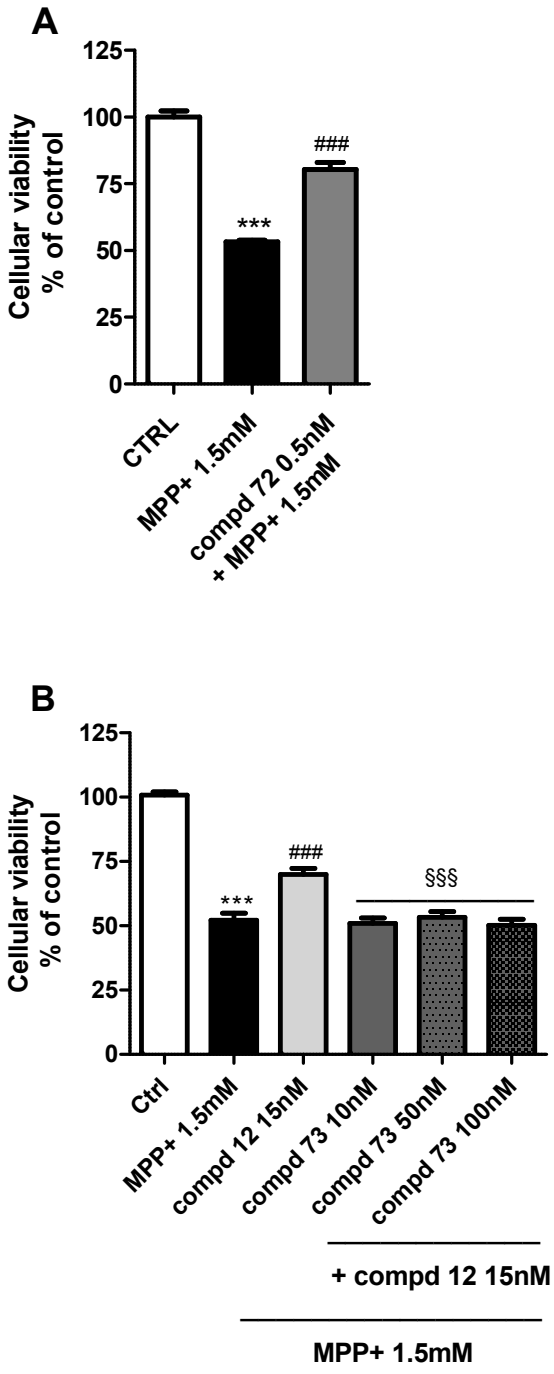


**Figure 3.** Reference $hA_{2A}$ antagonist **72**-induced neuroprotection against $MPP^+$ toxicity in SH-SY5Y cells (panel A). Neuroprotection induced by the $hA_{2A}$ antagonist **12** is lost by the coadministration of the selective $hA_{2A}$ agonist **73**. SH-SY5Y cells were treated for 24 h with 1.5 mM $MPP^+$ in absence and in presence of 15 nM of compound **12** and different concentrations of the agonist **73**, from 10 to 100 nM (panel B). Cell viability was evaluated by using CellTiter-Glo® luminescent assay. Data are expressed as mean of three independent experiments. ***P <0.001

compared with control, ###P<0.001 compared to $MPP^+$ 1.5 mM, §§§P<0.001 compared with $MPP^+$ 1.5 mM + **12** 15 nM.

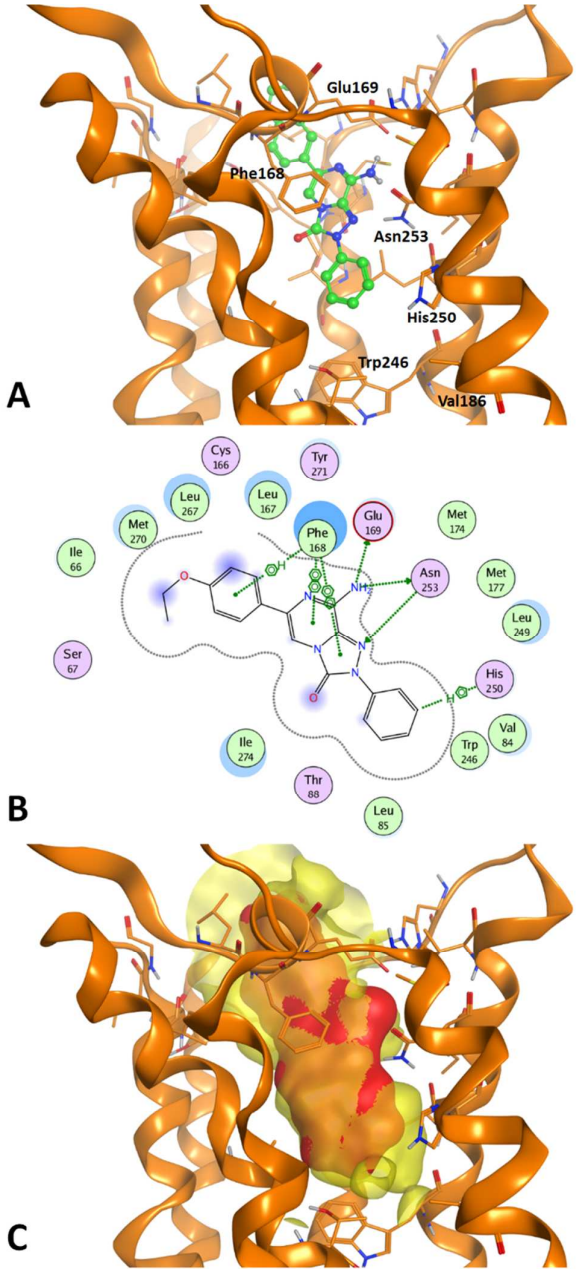


**Figure 4**. **A**. General binding mode of the synthesized compounds at the $hA_{2A}$ AR (pdb: 4EIY) binding cavity, with indication of some key receptor residues. **B**. Schematic description of the ligand-target interaction (built with MOE software). **C**. Molecular surface representation of the $A_{2A}$ hAR binding cavity (yellow) and the bound ligand (red) indicating the topological complementarity of the ligand and the cavity in the depth of the binding pocket.

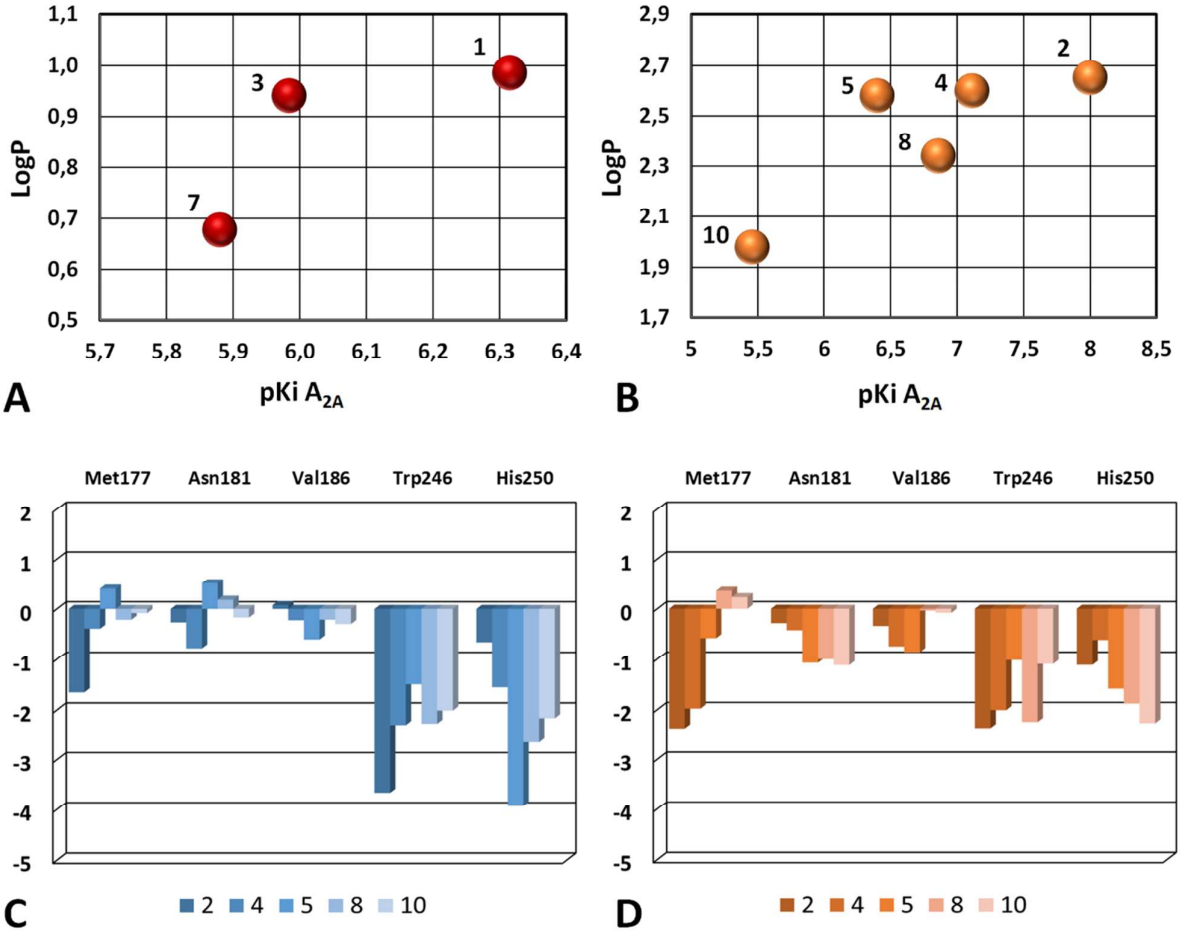


**Figure 5. A-B**. LogP versus $pK_i$ $hA_{2A}$ AR plot for the 6-methyl substituted compounds featuring an unsubstituted (**1**) or a para-substituted (**3** and **7**) 2-phenyl ring (panel A) and for the 6-phenyl substituted compounds presenting an unsubstituted (**2**) or a para-substituted (**4**, **5**, **8**, **10**) 2-phenyl ring (panel B). **C-D**. Ligand-target interaction energies calculated with the *IF-E 6.0* tool within MOE. The receptor residues in proximity of the 2-substituent were considered. Data are represented as kcal $mol^{-1}$. The blue histograms (C) describe the interaction energy values observed at the 4EIY $hA_{2A}$ AR crystal structure. At this structure, the interaction energy observed for the 2- substituent of compounds **2**, **4**, **5**, **8**, and **10** with the residues in proximity (see figure) is -6,16, -5.24, -5.11, -5.17, and -4.72 kcal $mol^{-1}$ (cumulative values), respectively. The orange histograms (D) describe the values observed at the 3EML $hA_{2A}$ AR structure. At this structure, the interaction energy observed for the same compounds with the residues in proximity is -6.48, -5.78, -5.12, -4.81, and -4.33 kcal $mol^{-1}$, respectively.

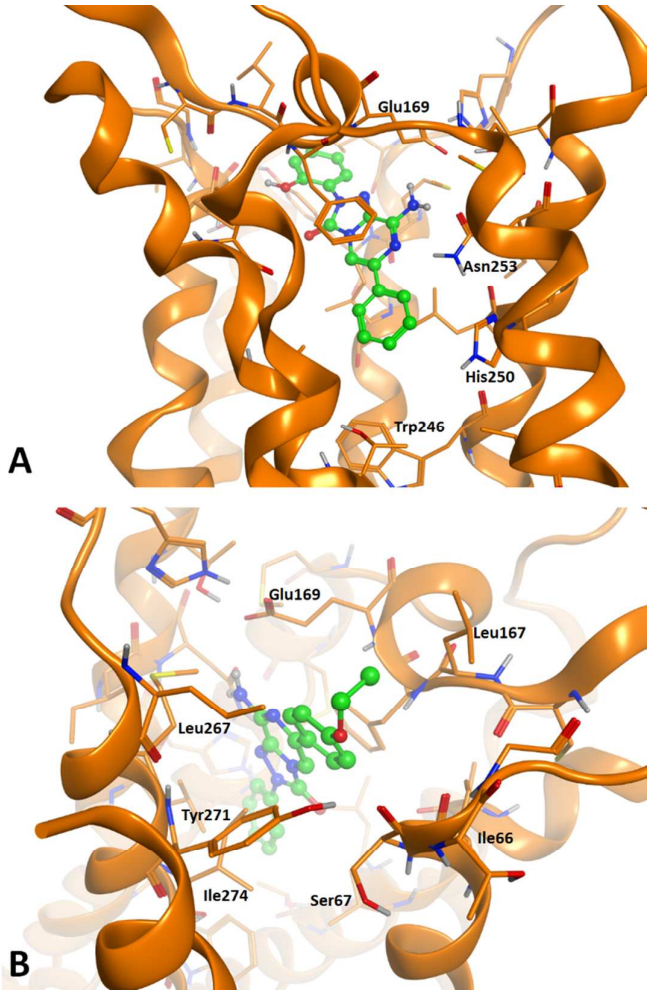


**Figure 6**. **A**. Alternative binding mode of the synthesized compounds at the $hA_{2A}$ AR (pdb: 4EIY) binding cavity, with indication of some key receptor residues. This binding mode was particularly observed for compounds presenting an ortho-substituted phenyl ring at position 2. **B**. $hA_{2A}$ AR residues located at the entrance of the binding cavity (pdb: 4EIY) and able to provide interaction with substituents on the $R_6$ aryl ring.

**Table of Graphic Content**

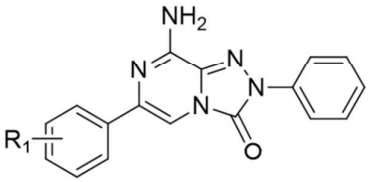


$R_1$= 4-$OCH_3$, 4-$OC_2H_5$, 4-$OCH_2$-C≡CH, 4-$OiC_3H_7$ } $hA_{2A}$ $K_i$ = 2.9-10 nM; $hA_1$, $hA_{2B}$, $hA_3$ $K_i$ > 30000